9

Dynamics of RF Micro-Mechanical Capacitive Shunt Switches in Coplanar Waveguide Configuration

Romolo Marcelli[1], Daniele Comastri[1,2], Andrea Lucibello[1], Giorgio De Angelis[1], Emanuela Proietti[1] and Giancarlo Bartolucci[1,2]
[1]*CNR-IMM Roma, Roma,*
[2]*University of Roma "Tor Vergata", Electronic Engineering Dept., Roma, Italy*

1. Introduction

Micro-electromechanical switches for Radio Frequency applications (RF MEMS switches)[1]-[4] are movable micro-systems which pass from an ON to an OFF state by means of the collapse of a metalized beam. They can be actuated in several ways but, generally, the electrostatic actuation is preferred because no current is flowing in the device nor power absorption has to be involved in the process.
The bias DC voltage signal is usually separated with respect to the RF signal for application purposes. Anyway, in the simplest mechanical model, a voltage difference V is imposed between the metal bridge, connected to the ground plane of a coplanar waveguide (CPW) structure, and the central conductor of the CPW, which also carries the high frequency signal. Under these circumstances, the switch will experience an electrostatic force which is balanced by its mechanical stiffness, measured in terms of a spring constant k. The balance is theoretically obtained until the bridge is going down approximately (1/3) of its initial height. After that, the bridge is fully actuated, and it needs a value of V less than the initial one to remain in the OFF (actuated) position, because contact forces and induced charging effects help in maintaining it in the down position. A general layout of the switch is diagrammed in Fig. 1a, with its simplified equivalent lumped electrical circuit. In Fig. 1b the cross-section of the device is shown, with the quantities to be used for the definition of the geometry and of the physical properties of the structure.
The actuation as well as the de-actuation are affected also by the presence of a medium (typically air, or preferably nitrogen for eliminating humidity residual contributions in a packaged device) which introduces its own friction, causing a damping, and altering the speed of the switch [5]-[7]. Several models are currently available to account for a detailed treatment of the damping, including also the presence of holes in the metal beam [8]-[11]. Moreover, the damping modifies the natural frequency of oscillation for the bridge. In particular, the actuation and de-actuation mechanisms will be consequently affected, leading to *simple oscillations* (no fluid damping contribution) or *damped oscillations* (fluid contribution) up to *over-damping* for particular values of the bridge dimensions or material properties. Experimental problems related to the dynamic characterization of

electrostatically actuated switches have been also considered elsewhere to predict and interpret experimental results [12]. Vibrations and damping are key issues in specific applications, and modeling as well as experimental determination are needed [13]. Optical analysis is one of the most advanced techniques for the characterization of movable Microsystems [14][15]. Other contributions to the motion of the switch are given by the repulsive "contact forces" of the bridge with respect to the plane, when it is already actuated or very close to the plane of the CPW, i.e. close to the substrate. They are due to the interaction between the two surfaces and to the local re-arrangement of the charges. The van der Waals force having an attractive effect has to be also included [5][7]. Both last contributions are, of course, very important when the bridge is close to the bottom RF electrode, in contact with the dielectric used for the capacitance needed to get the best RF isolation for the switch, and close to the actuation pad surface. It is difficult to manage the theory involving all of these contributions, and usually a phenomenological approach is followed, trying to individuate the most important parameters useful to describe the required mechanical and electrical response. For instance, higher is the ratio between the bridge thickness and the bridge length, higher will be the spring constant value and, consequently, the robustness of the switch.

In this chapter it will be demonstrated the usefulness of a fully analytical approach, as compared to the commercial software predictions, thanks to the implementation of all the contributions needed for describing the mechanical response of the double beam structure. In particular, further to predict the relevant quantities useful for the dynamical and electrical characteristics of the switch (actuation and release times, capacitance dynamics, …) a possible optimization of the structure will be proposed for no-contact actuation of the device, in order to minimize the surface and charging effects. One more contribution of this chapter is in the analytical derivation of the actuation voltage, depending on the strength of the applied voltage and the biasing area. This is very important when non-centered actuation voltage is applied, and simplified approaches are no more valid. In fact, this is the real case for devices implemented in RF configurations using the switch as a building block because, for application purposes, the RF and the DC paths have to be distinguished between them. Currently, many papers about the linear and non-linear dynamics of the switch are available in literature [3],[16]-[18] , including also possible collateral effects due to the Casimir force [19][20] or self-actuation mechanisms due to the level of the RF power [21]-[23]. Actually, power is a quantity to be carefully considered for potential applications in bolometers, and for this reason self-actuation was also proposed in nano- and micro-systems to get the power value from the actuation onset [24]. Nonlinear response of a double clamped beam under vibrations induced by RF fields have been recently studied, leading to the onset of chaos under specific solicitations and boundary conditions [25].

Analytical approaches have been also used for the circuital modeling of the switches, by fitting data [3][25][26] or deriving in closed form the expressions for the capacitance and for the resistors and inductors involved in the equivalent circuit [27][28]. Methods with EM considerations in circuit derivation have been discussed [30][31]. Inter-modulation products in the response of RF MEMS capacitors have been also investigated [32]. Thermal effects due to the power handling have to be considered as an additional issue.

A comprehensive study involving analytical and numerical predictions has been performed to obtain a full modeling of the electro-mechanical response of shunt capacitive micro-electro-mechanical (MEMS) switches for radio-frequency (RF) signal processing. The analytical approach was based on uni-dimensional equations, and it has been settled up for

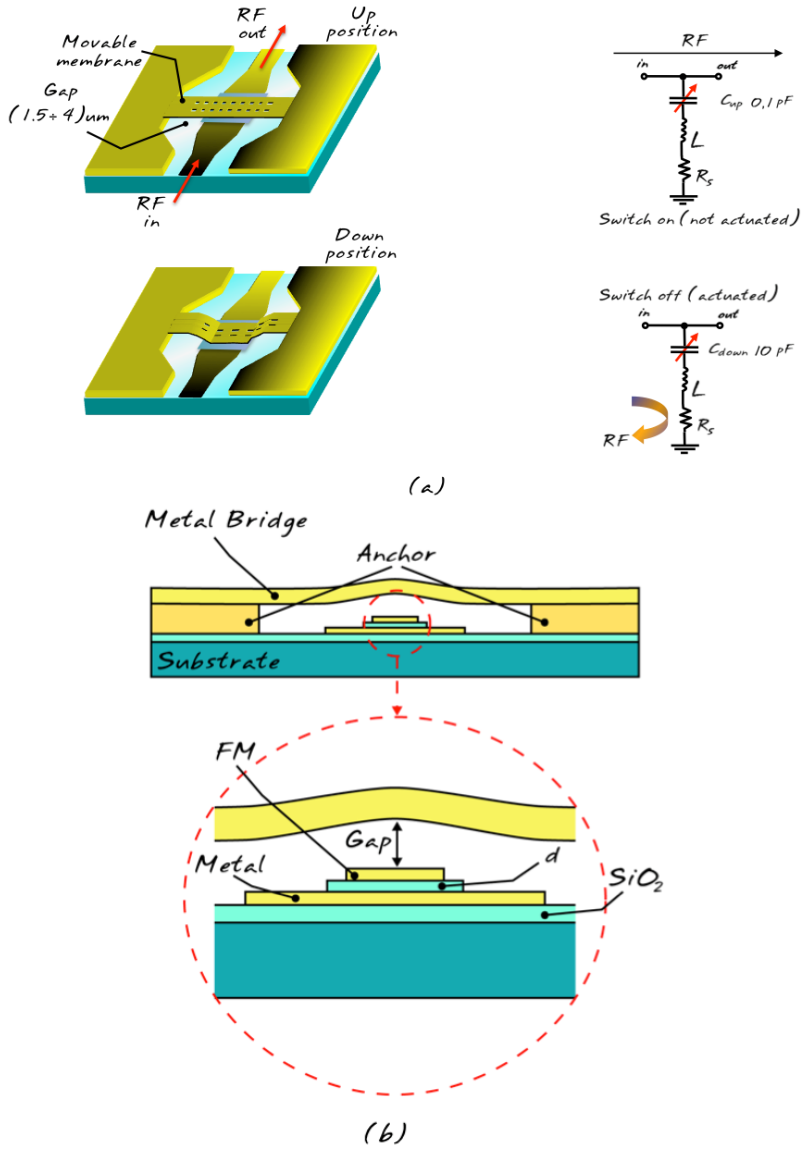

Fig. 1. (a) Schematic diagram of a RF MEMS capacitive shunt switch in coplanar configuration (left) and its equivalent circuit (right); (b) cross section of the switch structure, where the metal bridge is suspended by means of dielectric anchors on a multilayer composed by: (i) the air gap *g* with respect to+ (ii) a metal thin layer at a floating potential (FM) to be used for improving the capacitance definition in the down position, (iii) a dielectric layer with thickness *d* deposited onto (iv) the metal M of the central conductor of the CPW, and finally (v) the SiO_2 thermally grown layer onto the high resistivity silicon wafer.

studying the dynamics of RF MEMS shunt capacitive switches in a coplanar waveguide (CPW) configuration. The capacitance change during the electrostatic actuation and the de-actuation mechanism have been modeled, including the actuation speed of the device and its dependence on the gas damping and geometry. Charging and surface effects have been discussed, in order to select the physical and geometrical parameters useful for obtaining a reliable double clamped structure, eventually proposing simple configurations having no contact, thus minimizing surface and charging effects on the pads used for the electrostatic actuation. The model has been implemented by means of a MATHCAD program. Energy considerations have been included to account for the voltage necessary to maintain the switch actuated, by using a DC bias lower than the actuation voltage. The contribution of the charging mechanism has been discussed to describe both the maintenance voltage and the effects on the device reliability. Moreover, two- and three-dimensional models have been developed by using the commercial software package COMSOL Multi-physics, and they have been compared with the analytical and numerical results.
The above approach has been done for predicting the dynamical response of a capacitive shunt switch, but it is generally valid for resistive series as well as for capacitive shunt devices, because it has been implemented for a double clamped beam. Experimental findings confirm the validity of the proposed analytical approach, which is especially useful when a fast preliminary design of the device is needed.

2. One-dimensional model of the mechanical response of shunt capacitive RF MEMS switch

The equation which accounts for the most part of the above introduced physical mechanisms can be written as:

$$m\ddot{z} = F_e + F_s + F_p + F_d + F_c \tag{1}$$

where: $m = \rho A t$ is the bridge mass, computed by means of the material density ρ, the area A and the thickness of the bridge t; $F_e = \frac{1}{2}\frac{\partial C}{\partial z}V^2$ is the electric force due to the applied voltage V and to the change of the capacitance along the direction of the motion z; $F_p = -k[z-(d+g)]$ is the force due to the equivalent spring characterized by its constant k, acting against the electrical force to carry back the bridge to the equilibrium position; $F_s = -k_s[z-(d+g)]^3$ is the nonlinear stretching component of the spring constant [3]; $F_d = -\alpha\dot{z}$ is the damping force due to the fluid, dependent on the bridge velocity $\dot{z}$ and on the damping parameter α, which, in turns, is related to the geometry of the bridge and to the viscosity of the medium; F_c is the contact contribution, which can be divided in the van der Waals and surface forces, the first acting as attractive and the second one as repulsive, with a possible equilibrium position at a given distance from the bottom electrode of the switch [5].
The total capacitance of a shunt capacitive MEMS switch can be described in terms of two series capacitors, each of them having its own dielectric constant. This is only a formal way to approach the problem, because the intermediate plate is a dielectric interface and not a metal one. From the above considerations, and with reference to Fig. 1b, the total capacitance will be:

$$C(z) = \frac{\varepsilon_0 \varepsilon_r A}{d + \varepsilon_r (z - d)}; \qquad z \in [d, \quad d + g] \tag{2}$$

Where ε_0=8.85×10^{-12} is the vacuum dielectric constant in MKS units and ε_r is the relative dielectric constant of the material covering the bottom electrode. The derivative of $C(z)$, to be used in the definition of the electric force $F_e = \frac{1}{2}\frac{\partial C}{\partial z}V^2$ is given by:

$$\frac{\partial C}{\partial z} = -\frac{\varepsilon_0 \varepsilon_r^2}{[d + \varepsilon_r (z - d)]^2} A \tag{3}$$

and Eq. (1) can be re-written as:

$$m\ddot{z} + k[z - (d + g)] + k_s[z - (d + g)]^3 + \alpha \dot{z} = -\frac{1}{2}\frac{\varepsilon_0 \varepsilon_r^2 A}{[d + \varepsilon_r (z - d)]^2} V^2 \tag{4}$$

which can be transformed in:

$$\ddot{\zeta} + \beta \dot{\zeta} + \omega^2 \zeta + \frac{k_s}{m}\zeta^3 = B(\zeta) V^2 \tag{5}$$

where:

$$\begin{aligned} \zeta &= z - (d + g) \\ \beta &= \frac{\alpha}{m} \\ \omega &= \sqrt{\frac{k}{m}} \\ B(\zeta) &= -\frac{1}{2m}\frac{\varepsilon_0 \varepsilon_r^2}{[d + \varepsilon_r (\zeta + g)]^2} A \end{aligned} \tag{6}$$

The spring constant k is a measure of the potential energy of the bridge accumulated as a consequence of its mechanical response to the electrical force due to the applied voltage V. An approximated definition of it for central actuation can be given by [16]:

$$k = K_1 \left(32 E w r^3\right) + K_2 \left[8\sigma (1 - \nu) w r\right] \tag{7}$$

where:

$$\begin{aligned} K_1 &= \frac{1}{2 - \left(2 - \frac{L_c}{L}\right)\left(\frac{L_c}{L}\right)^2}; \; K_2 = \frac{1}{2 - \frac{L_c}{L}} \\ r &= \frac{t}{L} \end{aligned} \tag{8}$$

L is the bridge total length, L_c is the switch length in the RF contact region (width of the central conductor of the CPW), w is the bridge width, before the contact region, which can be also an averaged value as an approximation of the real cases if a tapering is present, t is the Au thickness of the bridge. The other parameters are the Young modulus E, the residual stress σ and the Poisson coefficient ν. As well established, the Young modulus is an intrinsic property of the material, and specifically it is a measure of its stiffness [33]

The Poisson coefficient ν is a measure related to the response of a material when it is stretched in one direction, and it tends to get thinner in the other two directions.

σ is mainly related to the process for obtaining the mechanical structure, and it must be measured in the real case. Actually, σ is a measure of the stress which remains after the original cause of the stresses (external forces, heat gradient) has been removed. They remain along a cross section of the component, even without the external cause.

A new, and more accurate definition of k has been recently given [35] for the treatment of miniature RF MEMS switches. Actually, it turns out that [35]:

$$\begin{aligned} L_{nc} &= L - L_c \\ L_d &= L_{nc}/2 \\ k_{new} &= \frac{2Ewt^3}{L_d^3} + \frac{Ewtg^2}{L_d^3} + \frac{2\sigma(1-\nu)tw}{L_d} \end{aligned} \tag{9}$$

where k_{new} is the new definition of the spring constant, to be compared with that given in Eq. (8). Generally, $k_{new} > k$ and bridges shorter than 500 μm ca. are better approximated by the k_{new} definition, exhibiting higher actuation voltages.

A recent experimental approach was also adopted for evaluating the contribution of the spring constant and for modeling it on the base of nano-indentation techniques [35].

All the quantities previously introduced have to be re-defined because of the presence of holes in the released beam. The holes need to be used for an easier removal of the sacrificial layer under the beam, and for mitigating the stiffness of the gold metal bridge, i.e. for better controlling the applied voltage necessary for collapsing it, to have not values too high because of the residual stress.

In this framework, we have re-calibrated the material properties accounting for the holes distribution on the metal beam. Literature definitions [3][37] are generally accepted for analytically describing the effect of the holes by means of the pitch, i.e. the center-to-center distance p between the holes and the edge-to-edge distance l. The situation is explained in the Fig. 2. In this way, the *ligament efficiency* will be given by the term (1-(l/p)) and such a term will be used in this paper for evaluating the effective quantities which are decreased with respect to the original one. Following this approach, $\sigma_{eff}=\sigma(1-(l/p))$, while $E_{eff}=E(1-(l/p))$, $\nu_{eff}=\nu(1-(l/p))$.

For the effective mass, we preferred to use a definition based on the ratio between the area with and without the holes, thus obtaining $m_{eff}=m(A/A_0)$, where A_0 is the geometrical area of the beam and A is the effective one considering the presence of the holes. All the evaluations which will be shown in this chapter are based on the previously defined quantities, calculated accounting for their effective contribution, but they have been written without the *eff*-pedex, for the sake of simplicity.

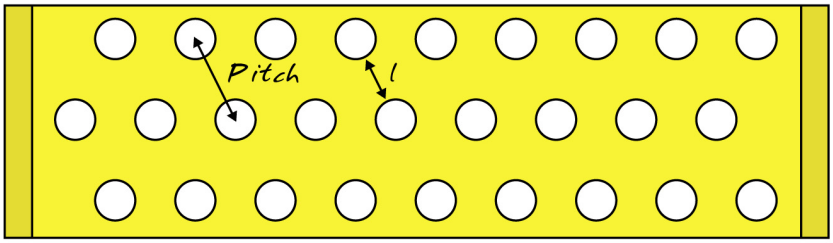

Fig. 2. Typical shape of a perforated beam used for RF MEMS double clamped switches. Holes are realized for facilitating the sacrificial layer removal and their position, number and dimensions are properly tailored depending on the application.

We included in this contribution a generalization of the mechanical evaluation for k. Actually, in the previous definitions, the spring constant is approximated accounting for a load in the center of the beam, but a constant load can be applied in different places along the beam, and the k value has to be calculated depending on the real position and extension of the applied force with respect to the bridge area. Two contributions are expected, the first one coming from the inertia moment of the beam and its Young modulus, and the second one having a technological origin due to the residual stress of the released bridge. Generalizing the equations introduced in literature about this topic [3] we can write:

$$\begin{aligned} k' &= -\frac{LEI}{2}\frac{1}{\int_{x1}^{x2} f(a)da} \qquad ; \quad f(a) = \frac{1}{48}\left(L^3 - 6L^2a + 9La^2 - 4a^3\right) \\ k'' &= \frac{L}{2}\frac{1}{\int_{x1}^{x2} g(a)da} \qquad ; \quad g(a) = \frac{L-a}{2\sigma(1-\nu)wt} \\ k &= k' + k'' \end{aligned} \tag{10}$$

Where $I = \frac{wt^3}{12}$ is the inertia moment classical calculation. Following the above definitions, we can effectively derive a k-value depending on the actuation position and on the size of the pads used to impose the voltage between the beam and the bottom electrode necessary for such a collapse, without approximations.
The threshold voltage, obtained by assuming that the mechanical structure collapses after trespassing the critical distance $(1/3)g$, is given by [3][17]:

$$V_{threshold} = \sqrt{8\frac{kg^3}{27\varepsilon_0 A}} \tag{11}$$

For the results coming from all the next simulations, we assume the following parameters for the bridge: L=600 μm as the bridge total length, L_c=300 μm as the switch length in the RF contact region (width of the central conductor of the CPW), w=100 μm as the bridge width, before the contact region, to be considered as an averaged value to fit the real cases if a tapering is present, w_S=100 μm for the switch width (transversal dimension of the switch, parallel with respect to the CPW direction), d=thickness of the dielectric material=0.2 μm, with dielectric constant ε=3.94 (SiO_2), t=1.5 μm for the gold bridge, ρ=19320 kg/m^3 for the

gold density, E=Young modulus=80×10^9 Pa, ν=0.42 for the metal Poisson coefficient and σ=18 MPa as the residual stress of the metal (measured on specific micromechanical test structures). The above defined physical quantities, as already discussed in the previous section, have been re-calculated because of the ligament efficiency.
An evaluation of k and of the actuation voltage has been given, according to the general geometry introduced in Fig. 3. In particular, holes with 10 μm diameter, side-to-side

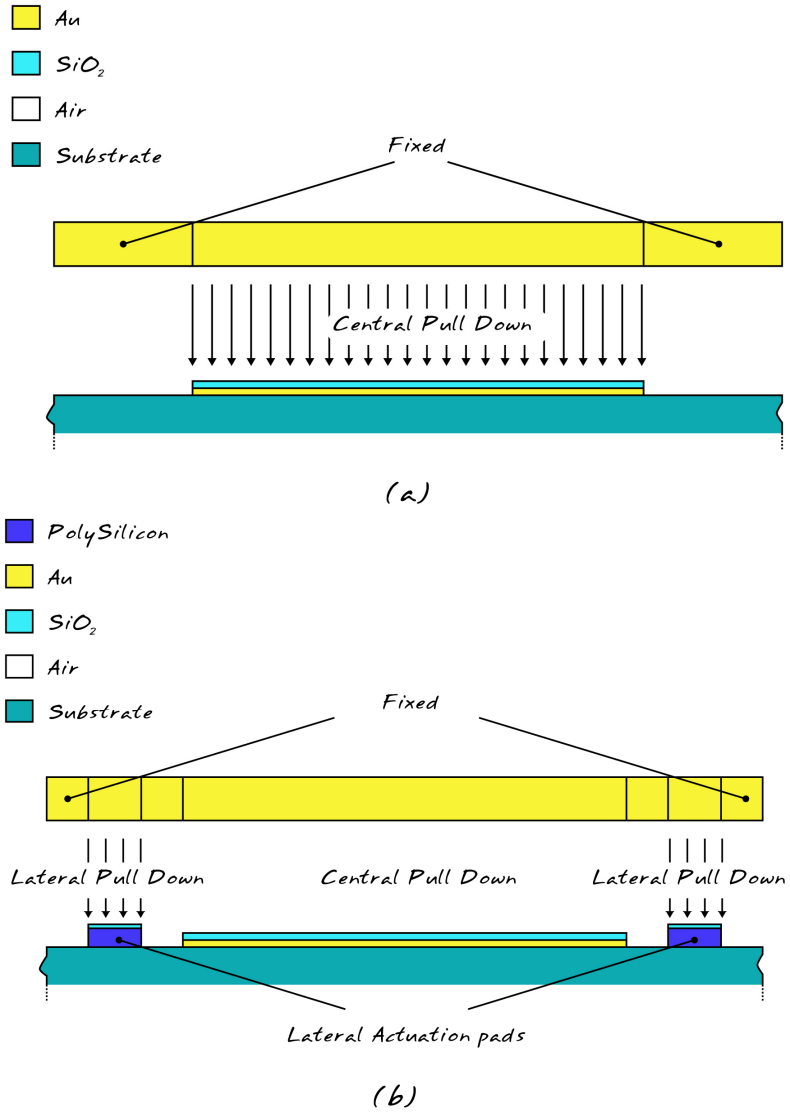

Fig. 3. Cross section of the geometry used for the simulation of the pull down of the metal beam: (a) by using the central actuation, and (b) by means of the lateral pads.

distance *l*=10 μm and center-to-center distance *pitch*=20 μm have been imposed. For the position of the actuation pads, we have chosen two possibilities: (i) central actuation, distributing the force over the entire area defined by the switch width and by the width of the CPW; and (ii) lateral actuation, by means of two poly-silicon pads 50 μm wide and long as the bridge width, centered with respect to the slot of the CPW. With reference to the following Fig. 3 and to Table I, the integration for obtaining the value of *k* to be used in Eq. (11) has been performed by choosing x_1 and x_2 by means of a coordinate system having the origin on the left side of the bridge. In this way, for the central actuation, $x_1=L/2$ and $x_2=(L/2)+(L_c/2)$; because of the symmetry of the analyzed structure, the integration is performed only on half of the length where the force is applied, and multiplied by a factor two (see Eq. (10)). For the lateral actuation, the same symmetry is invoked, and we have $x_1=(L/2)+(L_c/2)+d_{pad}$ and $x_2=(L/2)+(L_c/2)+d_{pad}+L_{pad}$, i.e. from the beginning to the end of the dielectric actuation pad for its entire length L_{pad}, distant d_{pad} from the edge of the central conductor of the CPW.
From the above data and from the *k*-values and actuation voltages V_{act} calculated for both actuation schemes (central and lateral) we obtained the results shown in Table 1:

	Central Actuation Eq. (7) and Eq. (10)	Lateral Actuation Eq. (10)
k [N m^{-1}]	10, 21	208
V_{act} [V]	13, 18	56

Table 1. Spring constant values and actuation voltages for the exploited geometry. It is worth noting that the voltage needed for the central actuation calculated by Eq. (7) is only an approximation with respect to that calculated by the exact Eq. (10); moreover the lateral actuation can be predicted only by using Eq. (10).

It is evident that the actuation requires a voltage applied in the center of the bridge much lower with respect to that needed at the sides of the double clamped structure. This is immediately understandable because of the higher value of the spring constant when the lateral actuation is used. Actually, in this modeling, the value of *k* is the parameter which accounts for the geometry used for the actuation of the switch.
Now, the particular and the general cases where voltage and damping are present or absent will be studied.

2.1 Case V=0, β=0

In this elementary case a small voltage can be applied just as a perturbation to the bridge, and after that the source is turned off, leaving the bridge moving in a non-dissipative environment. The cubic term due to the stretching is negligible and Eq. (5) is simplified in the well known equation of the harmonic oscillator:

$$\ddot{\zeta} + \omega^2 \zeta = 0 \tag{12}$$

The simple solution of Eq. (12) for the harmonic oscillator can be found by using a complex formalism, as:

$$\zeta(t) = \zeta_0 \exp[-i(\omega t + \varphi)] \tag{13}$$

and the real part will be:

$$\zeta(t) = \zeta_0 \cos(\omega t + \varphi) \tag{14}$$

with $\zeta_0 = \zeta_{0,\max} = \frac{1}{3}g$, and $\varphi = \frac{\pi}{2}$. The maximum value of the amplitude is given by the maximum allowed oscillation before a possible collapse induced by the applied voltage, and the phase is given by assuming an initial motion towards the bottom electrode. Then, the time dependence of the vertical coordinate to describe the maximum oscillation can be written as:

$$z(t) = (d+g) - \frac{1}{3}g\sin(\omega t) \tag{15}$$

This is a well established solution for the un-damped motion equation, but real cases always need the contribution of damped oscillations, which have been studied and will be presented in detail in the following sections.

2.2 Case V=0, β≠0

The presence of environmental intrinsic damping in the motion of the bridge will cause Eq. (5) to be re-written in the following way:

$$\ddot{\zeta} + \beta\dot{\zeta} + \omega^2\zeta + \frac{k_s}{m}\zeta^3 = 0 \tag{16}$$

As already mentioned, there are literature results concerning the correct analytical modeling of the medium in which a metal membrane is moving. By using a phenomenological approach, the effect of the damping can be modeled by defining a complex radian frequency as:

$$\omega' = \omega - i\Omega \tag{17}$$

where, usually but not necessarily, $\Omega << \omega$. The complex solution for Eq. (16) will be:

$$\zeta(t) = \zeta_0 '\exp[-i(\omega' t + \varphi)] \tag{18}$$

from which it can be inferred the relation between the natural radian frequency and that modified by the damping in the following form:

$$\omega' = \omega\sqrt{1 - \left(\frac{\beta}{2\omega}\right)^2} \tag{19}$$

It means that a decrease of the natural frequency is expected when the damping is present. In many physical situations, the condition $\beta/2\omega << 1$ holds. This will depend on the geometry of the bridge and on the intrinsic damping of the medium. The ratio $\beta/2\omega$ is a measure of the influence of the damping, and it will cause a different dynamical response [3][5][6]. The complex solution for the Eq. (16) with damping is:

$$\zeta(t) = \zeta_0 '\exp[-i(\omega' t + \varphi)]\exp(-\frac{\beta}{2}t) \tag{20}$$

It could happen that $\beta/2\omega<1$ or $\beta/2\omega>1$ depending on the damping and the resonant frequency values. Consequently, an oscillating response or an over-damping could be obtained. For this reason, the Real Part of the Complex Solution has to be taken:

$$\zeta(t)=\zeta_0'\mathrm{Re}\left\{\exp\left(i\left(\omega' t+\varphi\right)\right)\right\}\exp\left(-\frac{\beta}{2}t\right) \tag{21}$$

Analogously to the case of non-damped oscillations, and coherently with the maximum allowed oscillation before the possible collapse, it will be:

$$z(t)=(d+g)-\zeta_0'\mathrm{Re}\left\{\exp\left(i\left(\omega' t+\varphi\right)\right)\right\}\exp\left(-\frac{\beta}{2}t\right) \tag{22}$$

where $\zeta_0' \le \zeta_{0,\max}' = g/3$ and $\varphi=\pi/2$. Formulations of the damping term for a given geometry can be found in literature [3][5][7] and, as well established, the velocity of the bridge plays a key role together with the geometry and the viscosity of the medium. For such a contribution we can write [16]:

$$\begin{aligned}\alpha &= \frac{3}{2\pi}\mu\frac{A^2}{g^3}\\ \mu &= 1.2566\times10^{-6}\sqrt{T}\left(1+\frac{T_0}{T}\right)^{-1}\end{aligned} \tag{23}$$

A temperature dependence has been included, which accounts for the deformations induced by the change in the total length of the beam [3]. μ is the air viscosity, A is the full effective area of the bridge, including the ligament efficiency, T_0=110.33 K and T is the absolute temperature [3]. In our case, T=300 K. Different formulations appear in other papers [7], and it is the result of an approximation introduced in the equations used by us [3], but it does not change the conceptual approach to the problem. Other available results concern with the operation of the switch in harsh environment [38]. The response of the bridge is given in the following Fig. 4a. It is worth noting that by using the values imposed for the geometry of the exploited device, and considering that, by means of the definition of k given in Eq. (10), is valid the condition $\beta/2\omega>1$ for the central actuation, an over-damped flat solution is obtained in this case, without oscillations. On the other hand, for lateral actuation, as it is diagrammed in Fig. 3b, the beam exhibits a higher value for the spring constant, and the condition for the damping is $\beta/2\omega<1$, thus resulting in damped oscillations. See the results shown in Fig. 4b for a beam laterally actuated.

2.3 De-actuation of the bridge

The dielectric used for the RF MEMS switch capacitance is often SiO_2 or Si_3N_4, having ε_r=3.94 or 7.6 respectively, or any other dielectric material assuring a high C_{OFF}/C_{ON} ratio. Current results on high-ε materials are very promising for improving the isolation ratio [38]. The thickness of the dielectric material is usually in the order of tens to a hundred of nm, to provide, with the dimension of the gap g, the proper ratio of the capacitance between the ON (bridge up) and the OFF position (bridge down). By imposing g=2.8 μm and by using a 100 nm thick layer of SiO_2, from Eq. (2), the ratio is defined as:

$$R = \frac{d + \varepsilon_r g}{d} = 1 + \varepsilon_r \frac{g}{d} \approx \varepsilon_r \frac{g}{d} \tag{24}$$

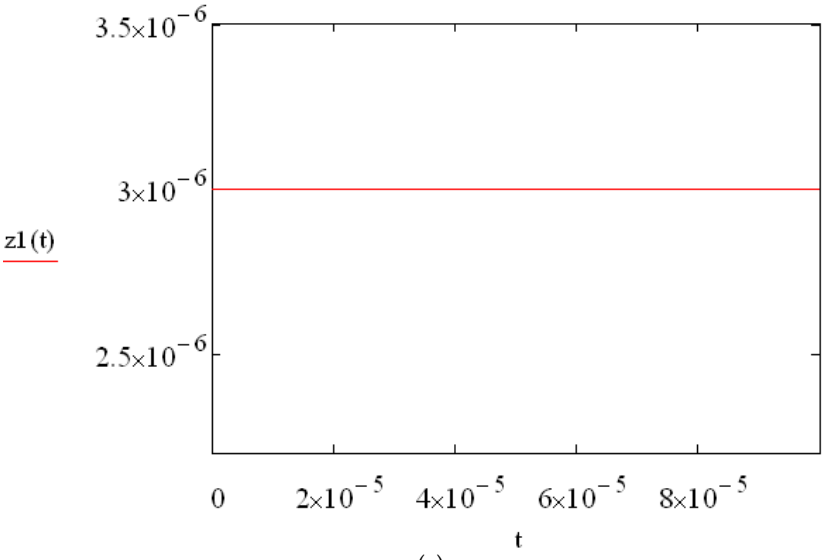

(a)

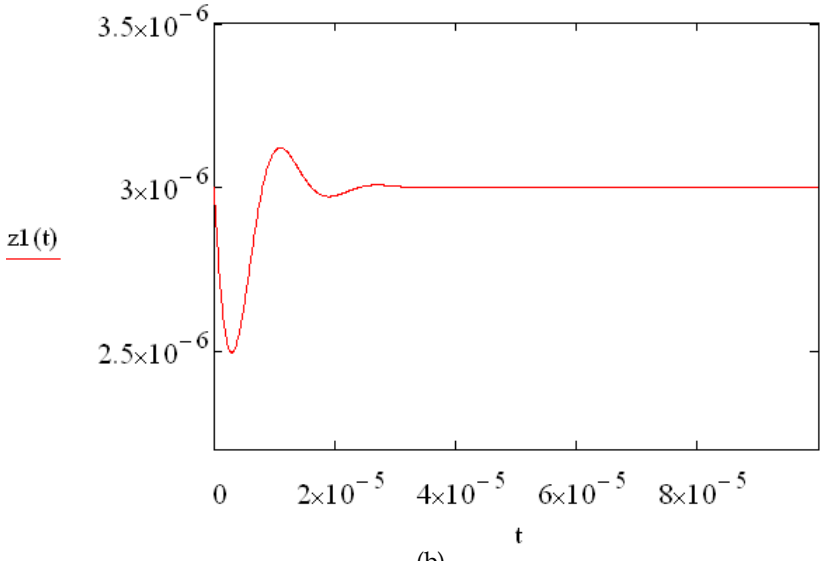

(b)

Fig. 4. Damped oscillations around the equilibrium position for (a) a centrally actuated, and (b) a laterally actuated beam. Higher values of *k* (lateral actuation) correspond to enhanced oscillations before obtaining again the equilibrium position. The time t is in sec and the vertical coordinate is in m.

where the last equation is valid in most practical cases, being $\varepsilon_r (g/d) >> 1$. In our case, the nominal ratio is $R \approx 56$ for the above imposed values of the parameters useful for describing the bridge mechanics by using SiO_2. Actually, as it has been discussed elsewhere[28], the OFF position of the switch is not characterized by a completely flat bridge fully adapted to the bottom electrode, thus contributing to an isolation between the two states lower than expected, unless to use different technological solutions like the floating metal one[39]. In the case of de-actuation, the full solution can be deduced by using the following formulas:

$$z_{deact}(t) = d + g + \zeta_0 \,\mathrm{Re}\left\{\exp\left(i\omega' t\right)\right\}\exp\left(-\frac{\beta}{2}t\right)$$
$$\zeta_0 = -g \tag{25}$$

All of the above described analytical solutions of the motion will involve a dynamical response of the capacitance *C*, which shall change according to the variation of *z*. Some detailed plots for the change of the capacitance as a function of time will be presented as a novel contribution with respect to the purely mechanical considerations. This is very important in the evaluation of the transient times useful to define the effective response and recovery times of the RF MEMS devices.
In the following Fig. 5 and Fig. 6, an example of the de-actuation response and of the *C*-response are shown, quite in agreement with similar results obtained elsewhere[29] but in this case we want to stress the extension of the analytical approach to the lateral actuation mechanism.

2.4 Actuation of the bridge

The actuation process is in principle more complicated, because the computation should involve the presence of the external force and of the contact forces when the bridge is very close to the contact area with the substrate. At a first approximation, without including the above contributions, we can write: $\zeta(t) = \zeta_0 '\exp[-i(\omega' t + \varphi)]\exp(-\frac{\beta}{2}t)$, which will lead to:

$$z_{act}(t) = d + \zeta_0 \,\mathrm{Re}\left\{\exp\left(i\omega' t\right)\right\}\exp\left(-\frac{\beta}{2}t\right)$$
$$\zeta_0 = g \tag{26}$$

This is the solution for the full equation with the initial conditions given by $z(0)=d+g$, i.e. with the bridge in the up position, pushed down by a voltage over the threshold. Actually, only positive values are allowed, because of the constrain due to the presence of the substrate. In particular, the solution for the actuation $z_{act}(t)$ will be:

$$z_{act}(t) = d - g\,|\,\mathrm{Re}\left\{\exp\left(i\omega' t\right)\right\}\,|\,\exp\left(-\frac{\beta}{2}t\right) \tag{27}$$

Intuitively, it means that the beam is expected to bounce before the full, final collapse, and the bridge will attempt to restore its initial position, but the applied voltage will force it to

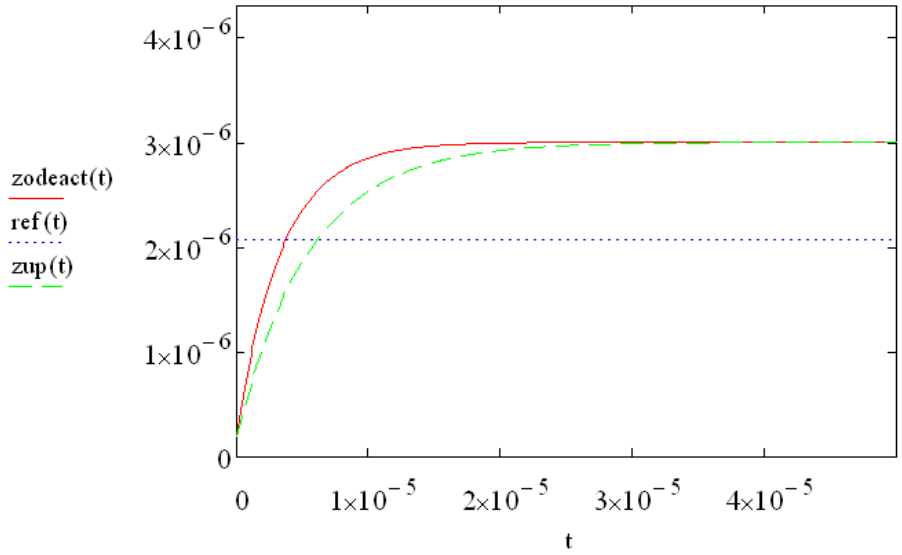

(a)

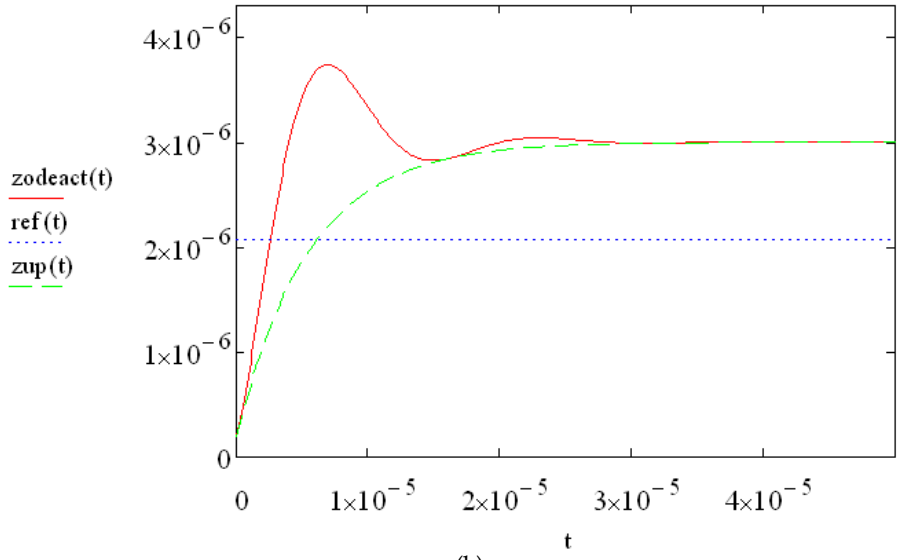

(b)

Fig. 5. De-actuation Vs time for the shunt switch used as an example (1.5 μm thick). The dashed curve (zup) accounts only for the exponential restoring mechanism, while the full one (zodeact) accounts also for the air damping. The dotted curve (ref) is the 1/3 limit of the gap for the collapse of the bridge. In (a) the central actuation is simulated, while in (b) it is shown the response for the lateral one.

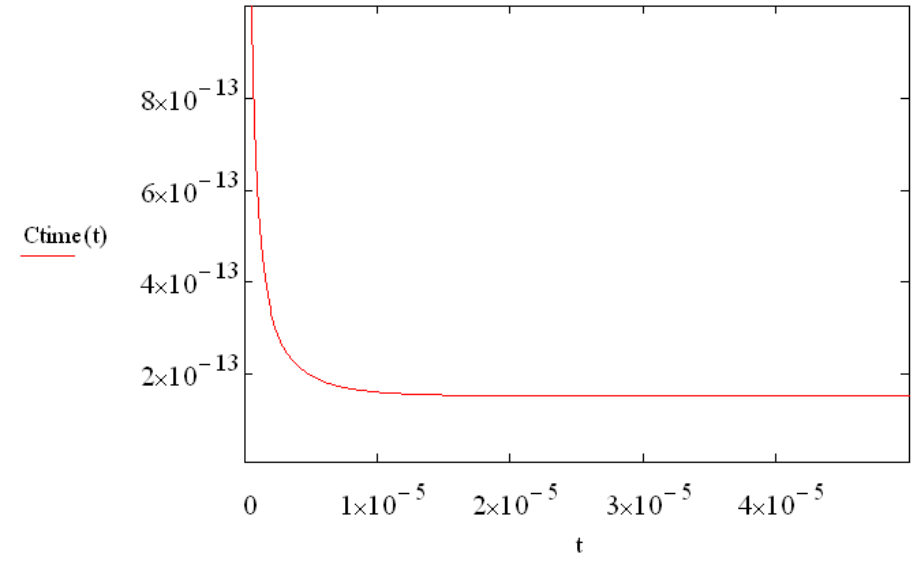

(a)

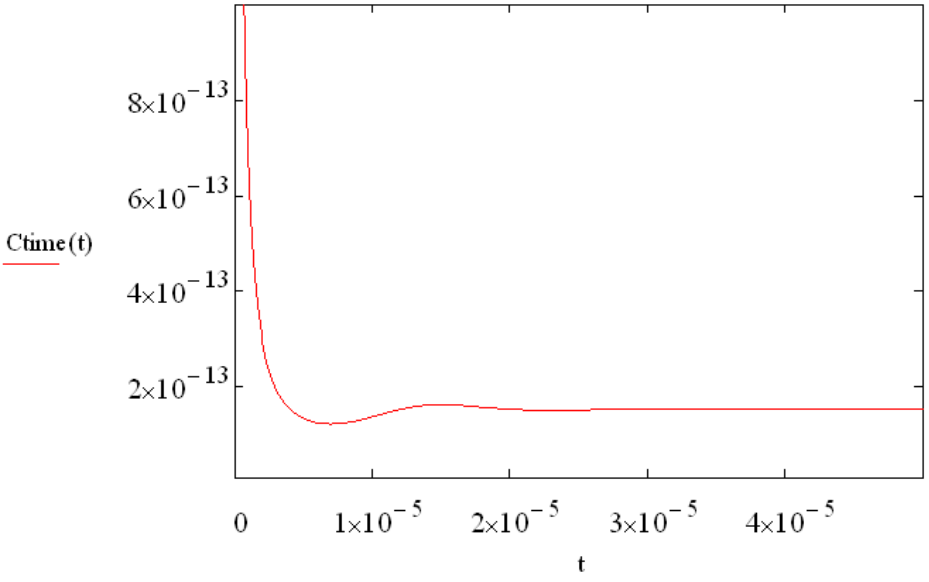

(b)

Fig. 6. Change of the capacitance Vs time for the RF MEMS switch (Ctime), in the case of (a) central actuation and (b) the lateral one.

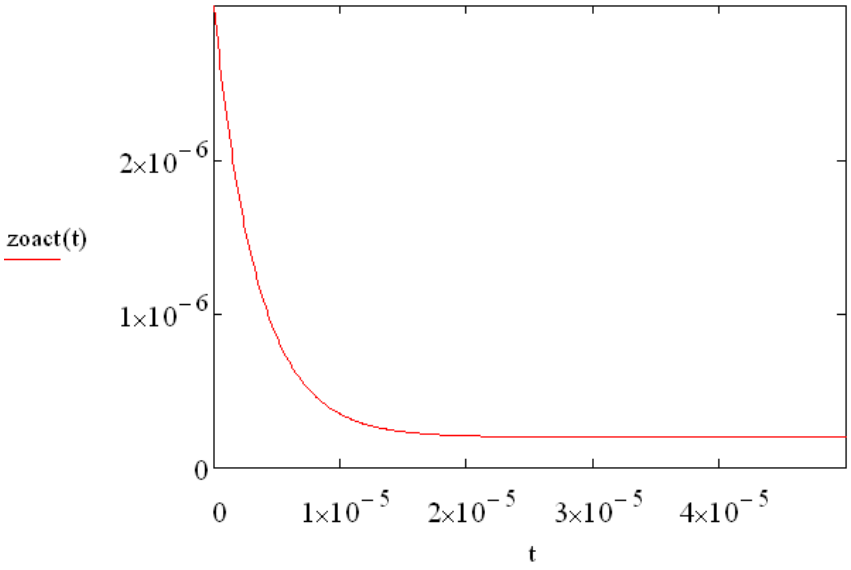

(a)

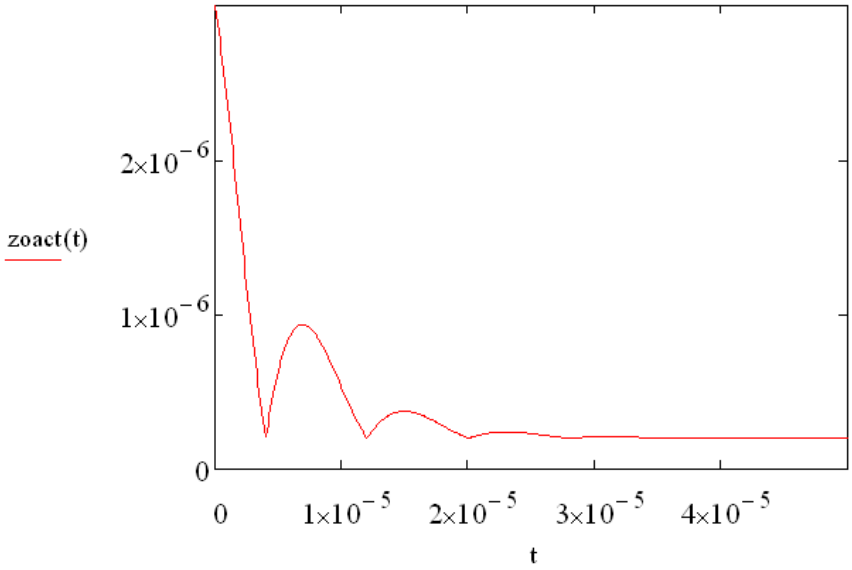

(b)

Fig. 7. Actuation of the bridge without accounting for contact forces. The curve (z_{oact}) is used to describe: (a) the central actuation for the 1.5 μm thick beam and (b) the lateral one. It is worth noting the number of bounces before the onset of the full actuation.

stay down. So far, the damped oscillation is due to the analytical solution of the motion equation, corresponding to a possible bounce before the full actuation of the bridge. Following this approximation, we shall have the situation depicted in Fig. 7a and 7b. It is worth noting that only for a high value of k, like it is for the lateral actuation, the bouncing effect is enhanced, while for the central one no bounces are expected for the imposed geometry. In fact, the condition $\beta/2\omega < 1$ is valid only for the lateral actuation, while it is $\beta/2\omega > 1$ for the central one, characterized by an imaginary solution and by over-damping. Of course, a compromise has to be chosen between the required actuation speed of the switch and its robustness and lifetime. It has also to be considered that the beam will be stressed more times when it is thicker, because also in this case we get an increase in the value of the spring constant and of the number of possible bounces, but a thin beam could be less reliable because of the experienced fatigue. A similar situation is obtained when you will have higher values for the residual stress, contributing again in the stiffness of the beam.
On the other hand, at least for a limited time, the van der Waals and contact forces will try to maintain the bridge in the DOWN position, introducing additional corrections. This situation is well described in other papers[18], where a solution similar to that presented in Fig.7 is given by studying an ohmic switch. Because of this effect, it is also claimed that a reliability analysis based on the nominal number of actuations is not correct, because it should include the effective number of bounces before the full actuation, each of them contributing to the fatigue of the beam.

3. Energy considerations and switching times

In this section we shall derive useful formulas for the evaluation of the switching times, based on energy computations. The electrostatic energy given by a voltage generator to a capacitive shunt switch in the ON state (UP position of the bridge), at the threshold for the electrostatic actuation, is given by:

$$E_{initial} = \frac{1}{2} C_{ON} V_{threshold}^2 \tag{28}$$

The threshold value $V_{threshold}$ of the voltage has been used to account for the full actuation of the switch when such a voltage is imposed. The system is non-conservative, and the final energy of the actuated beam (corresponding to the value of the OFF capacitance) will be changed by the contact and dielectric charging contributions, which have to be greater than the restoring mechanical energy for maintaining the beam in the DOWN position:

$$E_{final} = \frac{1}{2} C_{OFF} V_{threshold}^2 + E_c + E_{charge} \geq \frac{1}{2} k g^2 + \frac{1}{4} k_s g^4 \tag{29}$$

Where C_{OFF} is the capacitance when the switch is in the OFF state (bridge DOWN), and $(1/2)kg^2+(1/4)k_sg^4$ is the mechanical spring energy including the stretching contribution. As an implementation of the treatment given in classical literature about this topic [3], we have included additional terms [5],[7] and the contribution coming from the charging of the dielectric [41]. In fact, when the bridge is in the DOWN position, two more effects have to be

studied: (i) the contact energy E_c (repulsive and van der Waals), and (ii) the energy due to the charging process of the dielectric E_{charge}. To maintain the bridge in the DOWN position, accounting also for the above two additional terms, a holding down voltage V_{min} less than the threshold one can be applied. In this case the balance is obtained between the mechanical restoring energy and the electrostatic energy for the capacitance in the OFF state, plus the contact and charge terms, as:

$$\frac{1}{2}kg^2 + \frac{1}{4}k_s g^4 = \frac{1}{2}C_{OFF}V_{\min}^2 + E_c + E_{charge} \tag{30}$$

And the maintenance voltage V_{min} can be written as:

$$V_{\min} = \sqrt{\frac{kg^2 + \frac{1}{2}k_s g^4 - 2\left(E_c + E_{charge}\right)}{C_{OFF}}} \tag{31}$$

i.e., V_{min} can be determined by the spring constant k, the gap g, and the value of the capacitance in the OFF state (C_{OFF}). An estimation of the terms like E_c and its dependence on the position of the bridge is available[5],[42]. When successive actuations are performed, and considering E_c as an offset contribution, E_{charge} will increase up to a value where the switch will remain stuck also for V_{min}=0, unless to choose properly materials and geometry for the uni-polar bias scheme. Actually, V_{min}=0 will correspond to the sticking of the bridge, i.e. when $kg^2 + \frac{1}{2}k_s g^4 - 2\left(E_c + E_{charge}\right) = 0$. The threshold voltage, obtained by assuming that the mechanical structure collapses after trespassing the critical distance (1/3)g, is given by Eq.(11)[3],[17]. In the cases studied in this paper, and by using the same geometrical and physical data defined for our test structure, the change from the definition of k for central actuation to that for the lateral one can correspond to more than doubling the threshold voltage. From the above Eq (31), simple considerations can be anticipated about the contribution of charging processes and possible sticking of the bridge. It is known that successive applications of the voltage correspond to an accumulation of charge in the dielectric and in an increase of the actuation voltage[43], with an asymptotic trend up to its maximum value[44],[45]. In fact, if it is not given time enough to the charges to be dissipated, they grow up to the maximum contribution allowed by the geometry and by the properties of the dielectric material used for the capacitive response (in the case of central actuation) or by the dielectric used for the actuation pads (lateral actuation). The substrate too, when it is oxidized for improving the isolation, is a source of charges.

The switching times can be evaluated by means of the capacitance dynamics. Actually, exception done for the oscillations superimposed to the exponential decay, the envelope of the z-quote when the threshold voltage is applied will describe the change of the capacitance up to the full actuation of the device. As an approximation, we can say that the switch is *actuated* when the capacitance is 90% of that obtained from the full actuation procedure. In Fig. 8 the curve containing the oscillations of the capacitance, the maximum value when the bridge is in the DOWN position, and the reference value corresponding to $0.9C_{max}$ are shown.

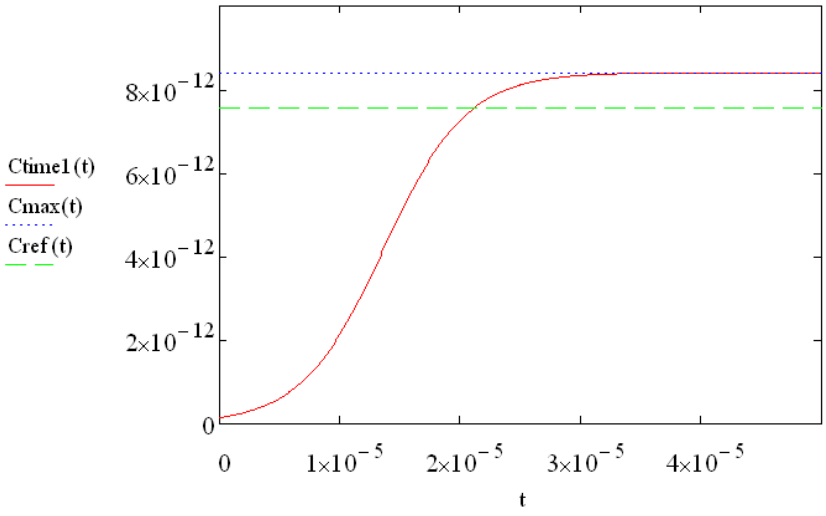

(a)

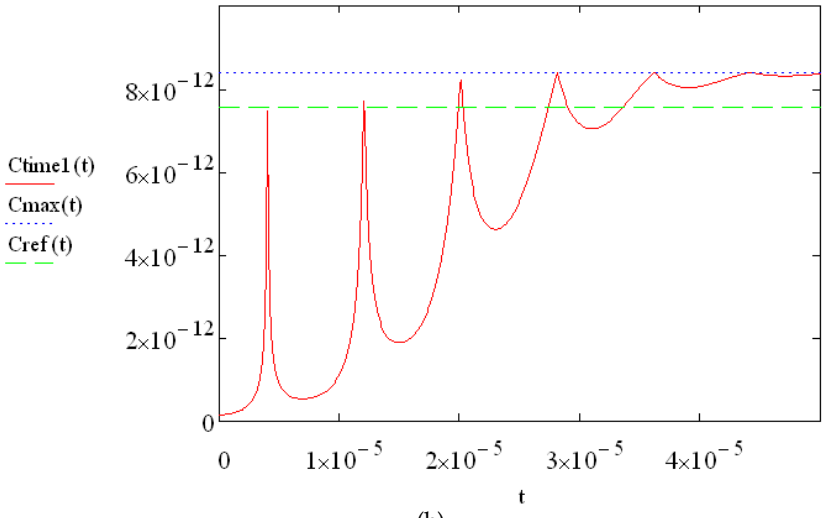

(b)

Fig. 8. Simulation of the actuation of the bridge. The curves describing the change of the capacitance (in F) during the actuation time (in s) are: (i) full curve, $C_{time1}(t)$, with the entire response by using *k*, (ii) flat full reference line C_{max}, i.e. the maximum value obtained when the switch is fully actuated, (iii) $C_{ref}=0.9C_{max}$. Both possible actuations are described: (a) central pull-down, and (b) lateral one.

It is worth noting from Fig. 8 the significant change of the oscillations induced by the different actuation choices. On the other hand, we can simplify the prediction for the actuation time by using the evolution of the envelope describing the actuation, which is written as:

$$C_{act}(t) = \frac{C_{OFF}}{1 + \varepsilon \frac{g}{d} \exp\left(-\frac{\beta}{2} t\right)} \tag{32}$$

The actuation occurs when C_{ref} crosses the envelope described by the previous Eq. (32). In formulae, after simple algebraic passages, it will be:

$$\tau_{act} = -\frac{2}{\beta} \ln\left(\frac{1}{9} \frac{d}{\varepsilon g}\right) \tag{33}$$

By using again the values used for the exploited structure, and assuming that the dielectric is SiO_2, it is ε=3.94 and $\tau_{act} \cong 35$ μs. The same evaluation can be done for the de-actuation, by using the results coming from Fig. 7 and the related analytical treatment. Actually, the evolution of the capacitance can be written, by using the exponential law for the envelope:

$$C_{deact}(t) = C_{ON} \frac{d + \varepsilon g}{d + \varepsilon g \left[1 - \exp\left(-\frac{\beta}{2} t\right)\right]} \tag{34}$$

From which it turns out, if $C_{deact}(\tau_{deact})=0.9C_{ON}$:

$$\tau_{deact} = -\frac{2}{\beta} \ln\left[\frac{1}{9}\left(1 - \frac{d}{\varepsilon g}\right)\right] \tag{35}$$

By using the same values imposed for the actuation, we obtain $\tau_{deact} \cong 12$ μs. It has to be stressed that both evaluations do not include the contact energy neither the charging contributions, so they should be corrected, but the order of magnitude should not change, exception done for some delay in the restoring mechanism when the switch is de-actuated, which should increase the τ_{deact} value.

The above evaluations concern with the response of the switch at the threshold voltage for the actuation. On the other hand, by increasing the applied voltage above such a threshold value, the velocity for the actuation can be increased too, as it can be obtained by considering the energy spent in the actuation process by performing the integral of the motion equation without accounting for contact or charging:

$$\begin{aligned}
&\int_{d+g}^{d} m\ddot{z}dz = m\int_{v(d+g)}^{v(d)} \dot{z}d\dot{z} = \frac{1}{2}m\left[v^2(d) - v^2(d+g)\right] = E_k = \int_{d+g}^{d} \left(F_e + F_m + F_d\right)dz \\
&\int_{d+g}^{d} F_e dz = \frac{1}{2}\left(C_{OFF} - C_{ON}\right)V^2 \\
&\int_{d+g}^{d} F_m dz = -\frac{1}{2}kg^2 \\
&\int_{d+g}^{d} F_s dz = -\frac{1}{4}k_s g^4 \\
&\int_{d+g}^{d} F_d dz = -\frac{\alpha}{\omega}\left[v^2(d) - v^2(d+g)\right]
\end{aligned} \tag{36}$$

Where E_k is the kinetic energy and E_d is the dissipated one, while $\omega = \sqrt{k/m}$. The dissipated energy has been calculated accounting for the dissipated power $P_d = F_d v = \alpha v^2 = \omega E_d$. The effect of k_s is marginal if we are far from the actuation region, but it becomes important close to the full collapse of the beam.
The above modeling is valid under the assumption that we are very close to the full actuation of the switch, but far enough to be obliged in considering the van der Waals and the contact contributions. The initial velocity of the bridge is obtained by $v(d+g)=v_{in}=0$ because it is at rest before the application of the voltage.
From Eq. (36) it turns out:

$$v_{act}(d) = \sqrt{\frac{(C_{OFF} - C_{ON})V^2 - kg^2 - \frac{1}{2}k_s g^4}{m + 2\frac{\alpha}{\omega}}} \tag{37}$$

i.e. the velocity v of the bridge subjected to the force imposed by means of the applied voltage is roughly linearly dependent on the applied voltage V. So far, Eq. (37) describes the velocity an instant before the bridge is collapsed. We can also write:

$$v_{act}(d) = \sqrt{\frac{(C_{OFF} - C_{ON})V^2 - kg^2 - \frac{1}{2}k_s g^4}{m + 2\frac{\alpha}{\omega}}} \quad \rightarrow \tag{38}$$

$$\rightarrow \left(\sqrt{\frac{(C_{OFF} - C_{ON})V^2 - kg^2 - \frac{1}{2}k_s g^4}{m}} \right)_{\alpha \rightarrow 0}$$

Actually, the dissipation causes a decrease in the velocity of the actuation by means of a term depending on a. It is like to substitute the mass of the bridge m with $m'=m+(2a/\omega)$. The dependence of the actuation velocity on the applied voltage V_a is shown in Fig. 9, where the dependence of v_{act} on V_a for the exploited device is presented.
When the bridge is released, no electrostatic force has to be included, and only the change of the potential energy and the contribution of the damping have to be considered for calculating the final velocity of the de-actuated beam, obtaining the result in Eq. (39) for the de-actuation velocity $v_{de\text{-}act}$, with $v(d)=0$ as the initial condition for the velocity:

$$v_{de-act}(d) = \sqrt{\frac{kg^2 + \frac{1}{2}k_s g^4}{m}} \tag{39}$$

Exception done for charging contributions.
From the analysis of the above figures, a significant change is expected comparing the results obtained by using the threshold value $V_{threshold}$ and a voltage higher than the

threshold one. The actuation speed is almost doubled by doubling the applied DC voltage. This enhances the dynamical response of the device, but it lowers the lifetime of the switch, tightly related to the mechanical fatigue induced by the electrostatic actuation. It is worth noting that, due also to the increased pull down voltage, the lateral actuation is faster than the central one.

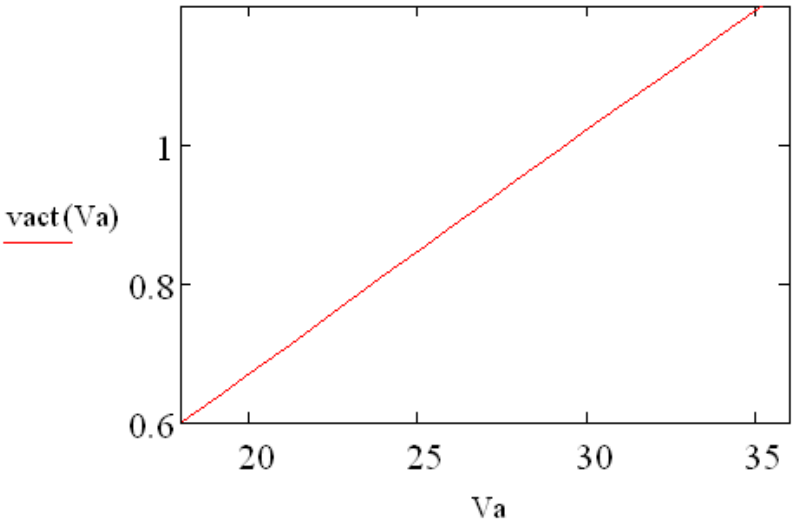

(a)

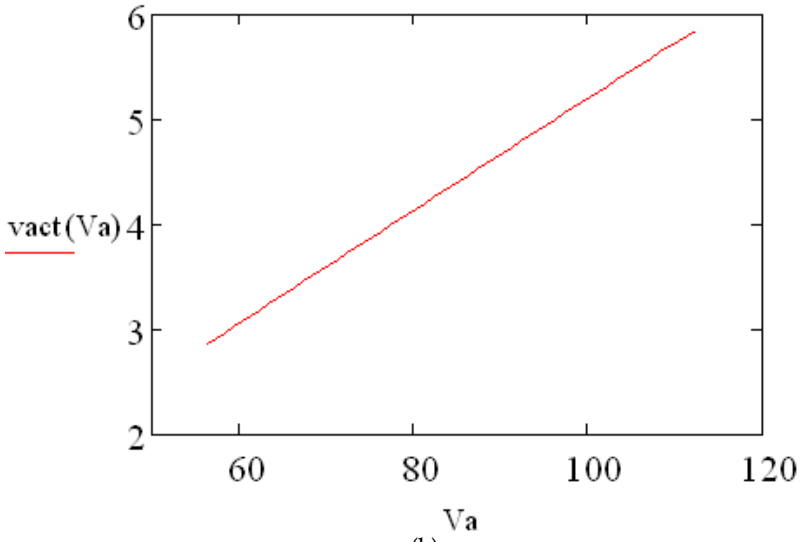

(b)

Fig. 9. Actuation speed v_{act} in m/s of the RF MEMS capacitive switch Vs the applied voltage V_a in volt, for the two simulated situations: (a) central actuation, and (b) lateral one.

Using capacitance dynamics considerations at the threshold voltage, we have assumed that the de-actuation and actuation times ($\tau_{de\text{-}act}$ and τ_{act} respectively) are the time values when the capacitance reaches the 90% of its final value. Such a definition is typically used to introduce the electrical response of a lumped circuit, and, by inverting the capacitance equation at these values, we get the phenomenological definitions for the characteristic de-actuation and actuation times. When energy and motion considerations are used, τ_{act} is the time for the full mechanical collapse of the beam and not just a time constant.
Concerning the de-actuation mechanism, by using the approach to lower the applied voltage for the maintenance of the bridge in the down position up to the V_{min} value, no dependence on V_a is expected.
For the actuation, the applied voltage is always present, and, by imposing a generic z-value in the integration for the energy spent in the actuation, it turns out that

$$v_{act}(z)=\sqrt{\frac{\left[C(z)-C_{ON}\right]V^2-k\left[z-(d+g)\right]^2-\frac{1}{2}k_s\left[z-(d+g)\right]^4}{m+2\frac{\alpha}{\omega}}} \tag{40}$$

To obtain the actuation time, the following equation can be used:

$$\tau_{act}=\int_0^{\tau_{act}}dt=\int_{d+g}^{d}\frac{dz}{v(z)} \tag{41}$$

and the applied voltage V can be imposed as a parameter. As a consequence, the actuation time for the exploited configuration is given in Fig. 10 by means of Eq. (41).
A similar result can be obtained for the de-actuation time, but it is independent of the actuation voltage, because the de-actuation occurs when the applied voltage is turned off.
Then, in our case $\tau_{de-act}=\int_0^{\tau_{de-act}}dt=\int_d^{d+g}\frac{dz}{v(z)}$ =18 μs ca.
In the case of the de-actuation the additional force due to the voltage is no more present, and the structure will respond only to the restoring forces dominated by the value of the spring constant.

4. Contact and van der Waals forces

The van der Waals and contact energies introduced in Eq. (29-30) and discussed in literature[5],[42] have attractive and repulsive effects respectively. From a physical standpoint they are due to dipolar contributions induced by atomic interactions. The energy associated with the two effects can be written in the form of the Lennard-Jones potential[42]:

$$E_c=4\delta\left[\left(\frac{\sigma}{R}\right)^{12}-\left(\frac{\sigma}{R}\right)^{6}\right]=\frac{B}{R^{12}}-\frac{C}{R^6} \tag{42}$$

Where B and C are positive constant values and R is the inter-atomic distance. Sometimes an exponential trend for the repulsive forces is preferred[42]. Because of the analytical formulation of such a potential, a bound state for the atoms is obtained for the minimum of

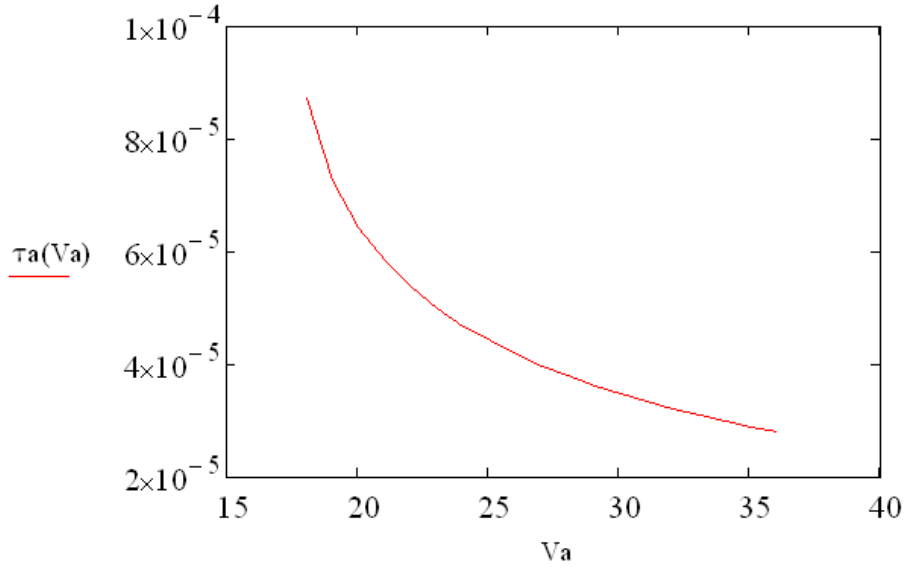

(a)

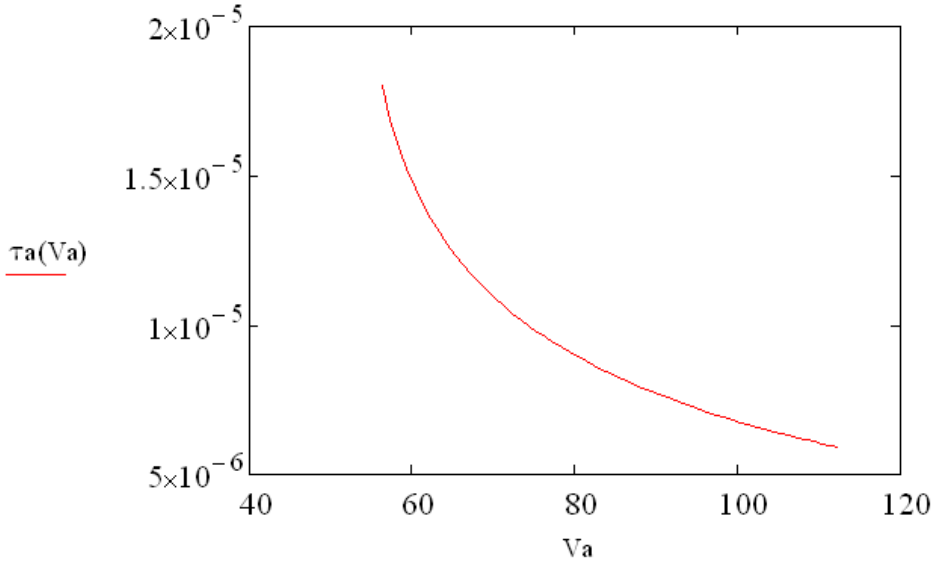

(b)

Fig. 10. Central (a) and lateral (b) actuation time τ_a as a function of the applied voltage Va for the studied device.

the energy, i.e. for the value of R vanishing the derivative of E_c. It will happen for $R/\sigma = 2^{1/6}$. Of course, all of the above considerations are free from the ambiguity of possible failures coming from adhesion related mechanisms induced by humidity, which can be present in both the processing and the operating conditions of MEMS devices.
A completely different approach has been followed elsewhere[45], where, further to the problems caused by the processing, the pinning due to inter-solid adhesion is analytically and experimentally treated for typical MEMS materials and structures. Also in this case a potential with a binding energy is derived, where the critical distance is associated with the contact area and the surface energy, and with the restoring force of cantilevers and double clamped bridges. The value for such a critical distance s^* for a cantilever is:

$$s^* = \left(\frac{3}{2} \frac{Et^3 h^2}{\gamma_s} \right)^{1/4} \tag{43}$$

It depends on the Young modulus E, the thickness of the beam t, the distance from the substrate h and the surface energy per unit area γ_s. In many cases the surface energy has to be fitted depending on the system, and the order of magnitude should be between 100 and 300 mJ·m^{-2}, but lower values have been also obtained in specific experiments on cantilevers and bridges. It is reasonable to assume a difference depending on the materials used for the contact region (metal-to-metal, metal-to-dielectric, …) and for other surface characteristics, like the roughness. The interfacial adhesion energy is given by[45]:

$$U_S = -\gamma_S w(l - s) \tag{44}$$

Being w the width of the beam, l the length of the cantilever before the contact area and s the length of the contact area with the substrate. The situation is illustrated in Fig. 7 of [45].
A particularly important result is the prediction of the distance at which a cantilever or a beam is detached, by using the definition of a *peeling bound number* N_p, where $N_p>1$ means that the beam can be free again after the contact with the substrate, while it remains in contact with the substrate for $N_p<1$. The results interesting for MEMS materials which can be used for beams to be electro-statically actuated are summarized in the following Table II[45].

Structure	N_p
Cantilever	$\frac{3}{8} \frac{Et^3 h^2}{\gamma_S l^4}$
Doubly clamped beam	$\left(\frac{128}{5} \frac{Et^3 h^2}{\gamma_S l^4} \right) \left[1 + \frac{4\sigma l^2}{21 Et^2} + \frac{256}{2205} \left(\frac{h}{t} \right)^2 \right]$

Table 2. Peeling bound numbers for cantilevers and doubly clamped beams. σ is the residual tensile stress. l is the full length of the suspended structure, either the cantilever or the doubly clamped beam.

By using the values for the exploited shunt capacitive MEMS device and from [47] γ_s=0.06 J·m^{-2}, in a doubly clamped beam configuration, it turns out that $N_p \approx 1.42$ for our perforated 1.5 μm thick and 600 μm long beam. From a quick analysis of the quantities playing a role in the definition of N_p, it is worth noting that it is important to have a thick beam in order to

have an effective restoring force. By decreasing the thickness t the value of N_p will decrease too. Moreover, the Young modulus E should be increased, and an additional but less relevant contribution comes from the increase of σ. In conclusion, a mechanically strong structure would be less influenced by the surface adhesion forces.
Some metals like Pt have a good E-value but they are less robust under continuous solicitations. Some others, like Tungsten Carbide, are very hard, but compatibility with standard CMOS processes and integration with microelectronics have to be fully demonstrated. Recent and promising results about molybdenum are available[34]. Materials selection properties are, in general, a hot topic for RF MEMS applications [48]. The threshold value for the actuation voltage is affected by E, which enters the definition of the spring constant k, and it could render unacceptable the voltage to be used for the actuation of the bridge. So far, a reasonable compromise involves the definition of the geometry and of the material to be used. Anyway, just doubling the value of E, i.e. not using Au but Pt, the actuation voltage passes from 29 volt to 30 volt ca. for the central actuation. It means that N_p passes from 1.42 to 1.53 ca. Since Pt is softer than Au, it is a negligible advantage and un-practical solution, because it will also cause problems in terms of repeated actuations of the bridge. An estimation of the van der Waals force has been also given by using a different formulation[49]. Repulsive forces, which can influence by a factor 2 or 3 the full evaluation of the contact contributions, have been neglected. As already discussed, such an interaction is responsible for binding in metallic contacts as well as in crystalline materials. The interaction energy due to van der Waals contribution can be written as:

$$U_{VDW} = -\frac{A}{12\pi d^2} \tag{45}$$

Where A is defined as the Hamaker constant (A=1.6 eV for Si [49], or A=4.4×10^{-19} J [47]) and d is the separation between the two surfaces. In the case of MEMS, at a microscopic scale, the roughness should avoid the adhesion, because it decreases the effectiveness of the surface contact, and residual gas molecules give a further contribution against a possible stiction [49]. As a further demonstration that it is quite difficult to have non-ambiguous results on the definition of the surface energy constant, other findings [18] have also to be considered, where γ_s=1.37 J·m^{-2} is given in the case of metal-to-metal contact in ohmic switches.
By using another approach [47], the value of γ_s can be obtained accounting that U_{VDW} when the surfaces are in contact between them corresponds to γ_s, i.e. $\gamma_s = U_{VDW}(d=d_0)$, where d_0 is the minimum distance between the two surfaces. Considering that the roughness due to the processing of the device is equivalent to cause a residual air gap in the order of 50-100 nm [51], we can estimate for our purposes

$$\gamma_s = 4.4\times10^{-19}/(12\pi d_0^2) = (1.17 \div 4.67)\times10^{-6}\ \text{J}\cdot\text{m}^{-2}.$$

If such a value can be considered reasonable for the MEMS technology, no limits on the full length of the bridge should be found. In any case, from all of the above considerations, and from the last ones concerning the roughness, the surface energy should play a minor or negligible role in the sticking of the cantilevers and doubly clamped beams. Humidity only should generate real problems of sticking for un-properly packaged devices

5. Charging effects and sticking

The maintenance voltage, i.e. the voltage V_{min} for holding down the bridge after the actuation, is lower than the threshold one. This will depend on the physics of the electrical contact. Actually, considering the results about surface forces commented in the previous paragraph, they should play no role in sticking, unless introducing other contributions depending on metal-to-metal diffusion and local welding due to aging, heating and power handling. So far, charging of the dielectric material used for the actuation pads should be the main effect in increasing the internal electrical field opposing the actuation one, which will depend on the charging of the device after many actuations [41],[43],[44],[45].
By using Eq. (31), and neglecting the contact contribution previously discussed, we shall have:

$$V_{\min} = \sqrt{\frac{kg^2 + \frac{1}{2}k_s g^4 - 2E_{ch\,\mathrm{arg}\,e}}{C_{OFF}}} \tag{46}$$

And the sticking will happen for $kg^2+(1/2)k_sg^4=2E_{charge}$. The energy accumulated by means of a charge trapping process will have no effect if a long time is left after the release of the bridge and before the successive actuations, but its contribution on V_{min} is not negligible since the first actuation.
A possible phenomenological approach for explaining the increase in the threshold value under a uni-polar scheme for the actuation voltage of an RF MEMS switch can be given accounting for the change induced in the electric field and, consequently, in the charge accumulated by dielectric layers.
Such an extra-voltage can be written as $\Delta V_{th} = d\,|\,\vec{E}_{ch}\,|$, where d is the thickness of the dielectric layer and E_{ch} is the electric field related to the accumulated charge, directed along the normal with respect to the dielectric plane. The charge will decay after the release of the bridge following an exponential trend, in such a way that:

$$\Delta V_{th}(t) = d\,|\,\vec{E}_{ch}(t)\,| = d\,|\,\vec{E}_{ch,0}\,|\exp\left(-\frac{t}{\tau_{ch}}\right) \tag{47}$$

Where τ_{ch} is the time constant of the decay process during the time t. By using a uni-polar scheme for the voltage to be applied to the MEMS switch (positive pulses only), and by imposing a pulse train with period T and pulse-width τ, successive actuations will be affected by a partial decay of the accumulated charge before the next pulse will actuate the switch again. Such an effect can be formalized by using the following equations:

$$\begin{aligned}
\Delta V_{th}^{(1)} &= d\,|\,\vec{E}_{ch,0}^{(1)}\,|\exp\left(-\frac{(T-\tau)}{\tau_{ch}}\right) \\
\Delta V_{th}^{(2)} &= d\left[|\,\vec{E}_{ch,0}^{(1)}\,|\exp\left(-2\frac{(T-\tau)}{\tau_{ch}}\right) + |\,\vec{E}_{ch,0}^{(2)}\,|\exp\left(-\frac{(T-\tau)}{\tau_{ch}}\right)\right] \\
\Delta V_{th}^{(3)} &= d\left[|\,\vec{E}_{ch,0}^{(1)}\,|\exp\left(-3\frac{(T-\tau)}{\tau_{ch}}\right) + |\,\vec{E}_{ch,0}^{(2)}\,|\exp\left(-2\frac{(T-\tau)}{\tau_{ch}}\right) + |\,\vec{E}_{ch,0}^{(3)}\,|\exp\left(-\frac{(T-\tau)}{\tau_{ch}}\right)\right] \\
&\cdots\cdots\cdots\cdots
\end{aligned} \tag{48}$$

In general, the amount of charge accumulated during successive actuations could be not constant, but we can assume, as a starting point, that $|\vec{E}_{ch,0}^{(1)}|=|\vec{E}_{ch,0}^{(2)}|=...=|\vec{E}_{ch,0}|$. It turns out in:

$$\Delta V_{th}^{(n)} = d\,|\vec{E}_{ch,0}|\exp\left(-n\frac{(T-\tau)}{\tau_{ch}}\right) \quad and$$

$$\Delta V_{th} = d\,|\vec{E}_{ch,0}|\sum_n \exp\left(-n\frac{(T-\tau)}{\tau_{ch}}\right) = d\,|\vec{E}_{ch,0}|\sum_n x^n = d\,|\vec{E}_{ch,0}|\frac{1}{1-x} = \tag{49}$$

$$= \frac{d\,|\vec{E}_{ch,0}|}{1-\exp\left(-\dfrac{T-\tau}{\tau_{ch}}\right)} \qquad where \quad x=\exp\left(-\frac{T-\tau}{\tau_{ch}}\right)<1$$

From Eq. (49) it turns out that a limit in the charge accumulation exists also in the simplified case of constant value for the induced electric field after each actuation.

The above approach is valid only in the case of a uni-polar scheme. When a bi-polar voltage is applied, it will result in induced electric fields having opposite polarization, and, independently of the decay time for the accumulated charge, the original situation will be partially restored after each application of the threshold voltage [44]. It is worth noting that the charge accumulated because of this mechanism sometimes needs very long times for the decay, and the dominant Poole-Frenkel effect is difficult to be prevented. Presently, studies are performed for optimizing materials and geometries, eventually using non-contact actuations. The previously defined quantity $d\,|\vec{E}_{ch,0}|$ gives the contribution necessary for evaluating the maintenance voltage after the first collapse of the bridge. Eq. (45) has to be re-written as:

$$V_{\min} = \sqrt{\frac{kg^2+\frac{1}{2}k_s g^4 - 2E_{ch\arg e}}{C_{OFF}}} = \sqrt{\frac{kg^2+\frac{1}{2}k_s g^4}{C_{OFF}} - \Delta V_{th}^2} = \tag{50}$$

$$= d\sqrt{\frac{kg^2+\frac{1}{2}k_s g^4}{\varepsilon A d} - |\vec{E}_{ch,0}|^2}$$

Where, from an energetic standpoint, $E_{ch\arg e} = (1/2)C_{OFF}\Delta V_{th}^2$

An evaluation of $|\vec{E}_{ch,0}|^2$ can be obtained by the knowledge of the charging mechanisms in the exploited dielectric. Results are available in literature about such a change in the voltage threshold by assuming that the Poole-Frenkel (PF) effect is the dominant one in the charge trapping of MEMS devices [51], taking into account that the current density due to the PF effect is $\vec{J}_{PF} = \sigma\,|\vec{E}_{ch,0}|$ .and σ is the conductivity of the material. The role of the above contribution in MIM capacitors and the dependence on the applied voltage and temperature has been studied elsewhere [52].

It has to be stressed that C_{OFF} will be quite different from the ideal one if residual air gap contributions have to be included, but in the case of floating metal solutions for the realization of shunt capacitive switches the C_{OFF} value is naturally obtained [28]. As the sticking induced by charging is one of the major problems in the reliability of RF MEMS

configurations, several solutions are currently studied for characterizing or suppressing such an effect [53],[54].

6. Bi-dimensional and three-dimensional mechanical simulations

Starting from the evaluations obtained by means of the uni-dimensional approach described in the previous sections, an extension to 2D and 3D structures has been performed by means of the COMSOL Multi-physics software package [55]. Commercial software begins now to be quite popular for simulating physical processes involving mechanical, thermal, high frequency and many other possible (and contemporary) solicitations for the exploited structure. In fact, only simple geometries can be efficiently simulated by using a uni-dimensional approach, thus estimating actuation times and actuation voltages without using long and complicated simulations with finite element methods. On the other hand, a full simulation is very important especially when the shape of the bridge is tailored in a not simple way. This happens when the cross section has not a constant width, or specific technological solutions, like metal multi-layers for the bridge, and dimples to help the electrical contact in the actuation area are realized. Holes are also present on the beam for improving the sacrificial layer removal and for lowering the spring constant, which is important when the stress induced by the technological process is not acceptable for practical purposes. In all of the above situations, effective quantities can be defined accounting for a re-definition of mass, contact area and beam width. Of course, small changes with respect to the ideal double clamped beam will have a small influence on the response of the entire structure, but more sophisticated geometries and technological solutions need a different evaluation. Moreover, software able to treat combined solicitations of the MEMS device has to be considered if the goal is the definition of a figure of merit for such a technology. For this purpose, 2D and 3D mechanical simulations have been performed to clearly state differences and advantages of such an approach with respect to the uni-dimensional one. An additional consideration is that the deformed shape of the actuated bridge, also in the case of simple geometries, is particularly useful for the prediction of the electrical properties of the device, which could be affected by parasitics for very high frequencies, starting form the millimetre wave range (F > 30 GHz). In the following discussion, parametric and electro-static simulations will be presented, with the aim to compare the central and the lateral actuation, and the expected shape of a simple fixed-fixed beam structure. As the threshold voltage $V_{threshold}$ is not dependent on the width of the bridge, because it is proportional to the ratio k/A between the spring constant k and the area A of the actuation region, the actuation of a bridge with no holes neither tapering along the width can be considered a 2D problem. Some 2D results are presented in Fig. 11-14, where the OFF state of the switch has been obtained by using a central actuation (DC signal along the central conductor of the CPW) or a lateral one by means of symmetrical pads. In both cases the electrostatic package implemented in COMSOL has been used, with a parametric simulation performed by changing the value of the applied voltage. A structure having the same dimensions imposed for the uni-dimensional treatment has been simulated: full length L=600 μm, width W=300 μm for the central conductor of the coplanar structure (corresponding to the bridge length in the actuation region), thickness t=1.5 μm for the bridge. The residual stress is again σ=18 MPa. The central conductor is Au, 0.1 μm thick,

covered by SiO_2, 0.2 μm thick. The bridge width is 100 μm, along the direction normal with respect to the 2D view. In the case of Fig. 11, the parametric force needed to get the fully deformed shape of the beam is given by $F = -kg$ = -46 μN, corresponding to a pressure of 1.5×10^3 N/m² ca. This is in agreement with the value obtained by using the 2D simulation. On the other hand, the nonlinearity of the mechanical problem allows for a full actuation when the structure begins to be unstable, i.e. when the applied force is sufficient to push the bridge down (1/3) of the gap. This happens at $z = 2(d+g)/3$ = 2 μm, corresponding to a mechanically simulated structure subjected to a force F = -15 μN and to a pressure of 500 N/m² ca. By calculating the value of $\partial C / \partial z$ when $z = 2(d+g)/3$ and substituting in $V = \sqrt{2F/(\partial C / \partial z)}$ obtained from the definition of the electrostatic force, the voltage V=20 volt is obtained for the threshold, thus demonstrating that the actuation of the bridge can be easily predicted by using the uni-dimensional approach. In this and in the following simulations holes are not included, but from the uni-dimensional simulations, it turns out that V=18 volt is obtained when holes are present, while V=20 volt is the expected threshold voltage for the structure with holes, i.e. only a 10% difference.

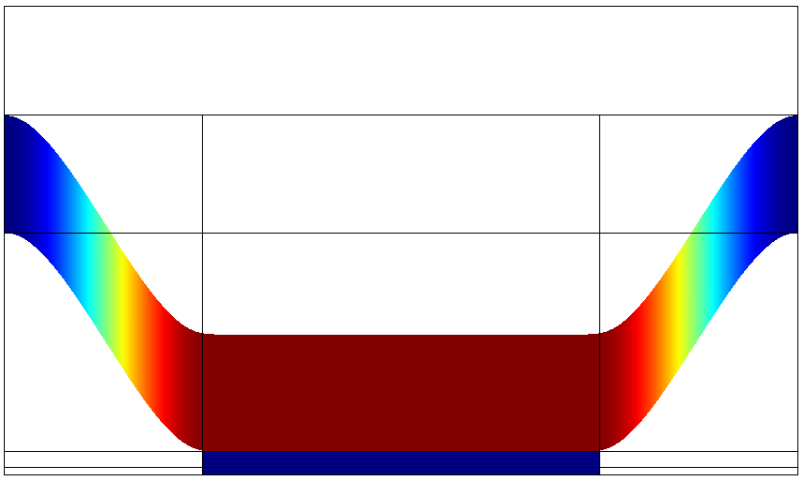

Fig. 11. 2D simulation for the central actuation of the MEMS switch (COMSOL simulation). A mechanical force per unitary area on the central conductor of the CPW has been applied as high as 1500 N/m² to obtain the full actuation.

From the result in the next Fig. 12, where the lateral actuation is imposed, it turns out that by properly choosing the shape and the dimensions of the structure, the actuation occurs without having the bridge touching the lateral pads. This could help in decreasing the charging effects for these devices, mainly due to the dielectric used onto the actuation pads, which dramatically affects their reliability in terms of the charge stored. Moreover, the necessity to separate the RF and DC paths is another important reason for preferring a lateral actuation in actual devices.

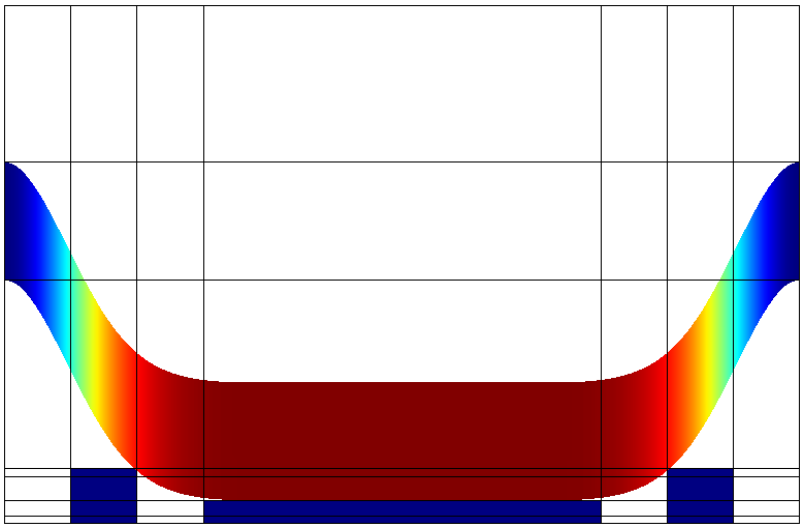

Fig. 12. Lateral actuation of the 2D structure (COMSOL simulation). The same force used for the central actuation was necessary for having a full collapse of the bridge, but applied on smaller lateral pads (50 μm width). A more uniform actuation is obtained, as evidenced by the colour intensity in the central part. Moreover, the beam is contact-less on the pads, which helps in minimizing the charging effects.

An example of the 3D response is given in the following Fig. 13 and Fig. 14, where the actuation has been performed by means of the same force used for the 2D case, with details about the full device. The result is coherent with the prediction performed by using the analytical approach and the 2D actuation. In fact, the mechanical force per unitary area imposed in the simulation for obtaining the full collapse of the bridge corresponds to a pressure of 1500 N/m^2 , i.e. to a force of 45 x 10^{-6} N applied onto an area of 300 x 100 x 10^{-12} m^2. This is the value of the mechanical restoring force applied in the centre of the double clamped beam, and by calculating again the value of $\partial C / \partial z$ when $z = 2(d+g)/3$ and substituting in $V = \sqrt{2F/(\partial C / \partial z)}$ the voltage V=20 volt is obtained also in this case. So, the actuation of the bridge can be easily predicted by using the uni-dimensional approach, also including rough evaluations about the holes contribution, but avoiding long term simulations, exception done for those structures where the distribution of the holes is very complicated or a significant shape tailoring is present and the analytical approach should be forced by the introduction of effective quantities not really matching the actual situation.
By properly choosing the dimensions and the materials, lateral actuation is possible with voltages in the same order of magnitude used for the central one, as from the comparison between the results coming from data in Fig. 13 and Fig. 14, with evidence for contact-less actuation.
Only in simple cases the presence of holes can be approximated by defining an effective stiffness for the metal beam. For the above reason, the 3D simulation is really useful, as already stressed, in the case of configurations which have a very peculiar shape. Also in the case of a moving mesh, i.e. a mechanical solver to be used for the dynamical response of the

device, many information can be already obtained from evaluations based on a fully analytical model, without involving cumbersome simulations. A real advantage in having a full 3D modelling of the device is in the combination of mechanical and RF predictions,

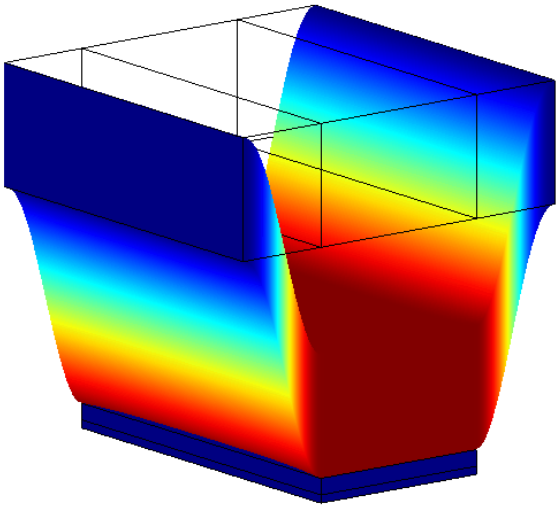

Fig. 13. 3D COMSOL simulation of the RF MEMS shunt capacitive switch in the OFF state (bridge in the down position), centrally actuated.

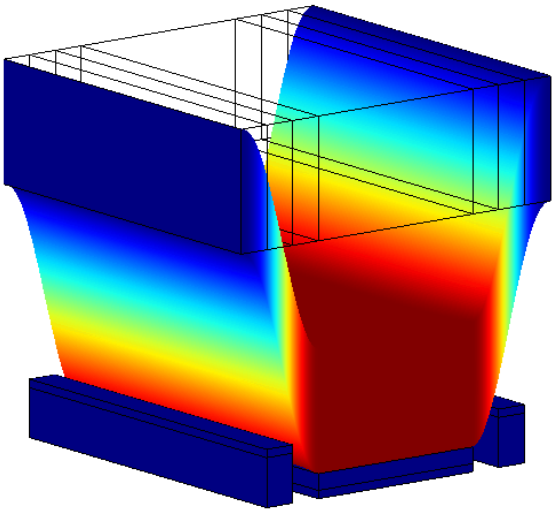

Fig. 14. 3D simulation of the RF MEMS switch in the OFF state (bridge in the down position), laterally actuated when the applied force per unitary area is F=1500 N/m^2. The deformation of the bridge is represented by the change in the colours, from the blue (at rest) to the red (fully actuated).

being based on the construction of the same geometry. Specifically, as it is the case of the COMSOL software package, thermal, power and charging effects could be considered in the same simulation environment. For the above reasons, this will be very useful to get a figure of merit for the RF MEMS technology based on different input conditions.
As a final demonstration of the validity of the proposed theoretical approach for the electro-mechanical analysis, one more simulation has been performed by means of the electrostatic force directly defined within COMSOL as $F_e = \frac{1}{2}\frac{\partial C}{\partial z}V^2 = \frac{1}{2}QE$

where Q is the charge and E is the electric field. The result is shown in Fig. 15, where the structure is pushed down (1/3) of the gap, before the final actuation occurs following the mechanical instability of the structure. It happens by imposing a voltage V = 22 volt ca., very close to the calculated threshold value by using the uni-dimensional approach.

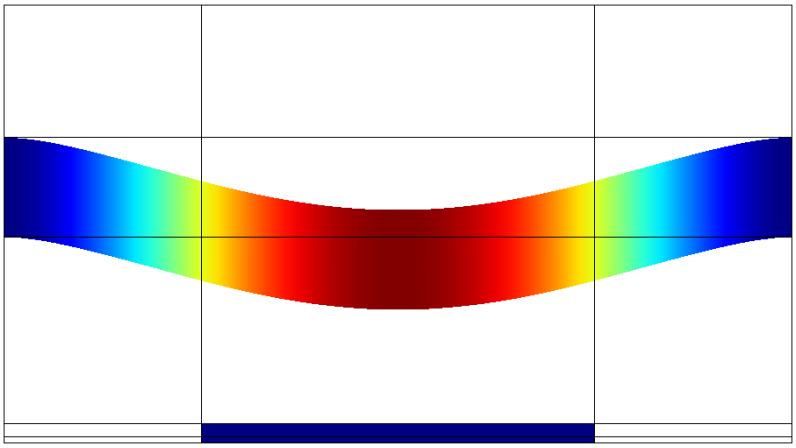

Fig. 15. Electrostatic 2D simulation for the exploited double clamped beam. V = 22 volt was necessary for having a movement of the beam close to (1/3) of the gap.

7. Technology, experimental results and discussion

An actual configuration having the same dimensions described in the previous sections has been realized and preliminary tested. A photo of the structure is given in Fig. 16. SU-8 polymeric sides have been realized by photo-lithography to be used as a support for both the ground planes of the CPW, and the suspended metal bridge. Silicon oxide has been deposited as a dielectric, and the actuation has been performed by means of the central conductor of the CPW.
The realization of double-clamped RF MEMS capacitive shunt switches has been performed by means of negative photo-resist SU-8 for the realization of the ground planes of the coplanar configuration, elevated with respect to the wafer, while positive S1818 photo-resist has been used as a sacrificial layer.
RF MEMS Switches have been manufactured on a 4 inch high-resistivity (ρ > 5000 ohm cm) silicon wafer <100> oriented, having a thickness of 400 μm. For the realization of the devices, a 4 mask sequence has been considered, and the entire fabrication process is sub-divided in five steps:

i. realization of the central conductor of the CPW.
ii. definition of the SiO_2 to be used for obtaining the capacitive configuration, with the aim of a high ratio in the ON/OFF states.
iii. creation of lateral supports made by SU-8 for the double-clamped structure. SU-8 2002 (Microchem Corp., USA) has been used for our purposes. In this configuration, polymer lateral pedestals are obtained, to be metalized for obtaining both the ground planes and the support for the suspended bridge.
iv. reduction of the sacrificial layer has been obtained by means of a purposely designed mask, in order to avoid peaks in the shape coming from the lithography, which act as discontinuities in the next metallization process.
v. as a final step, the switches are obtained by means of the release of the sacrificial layer by using a modified reactive ion etching (RIE) process.

Actuation voltages in the order of 20-25 volt have been obtained in different samples, almost in agreement with the expected value. A possible small under-evaluation of the gold membrane stiffness should be considered in the actual device. In fact, by imposing σ=25 MPa we obtain $V_{threshold}$=21 volt ca. for a uniform beam with the same dimensions and holes. Moreover, because of the stiffness the beam could be also a bit upward with respect to the expected flat geometry and an increased gap could favour and increase in the threshold voltage. Other possible sources of spread with respect to the predicted threshold voltage maybe due to non-uniformity in the Au deposition over the entire 4 inch wafer, and the successive electro-plating process.
An optical characterization of the manufactured device has been also performed, revealing both a good shape of the beam and the resolution of the holes, which have no residuals after the ashing process. Results are given in Fig. 16.

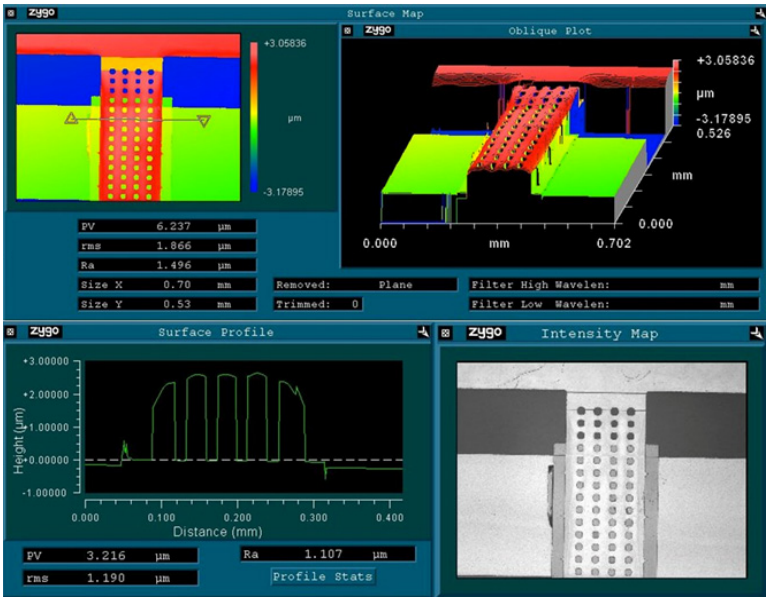

Fig. 16. Optical microscopy characterization of the RF MEMS switch realized by means of SU-8 photo-lithography with evidence for the optimized profile of the beam after the removal of the sacrificial layer.

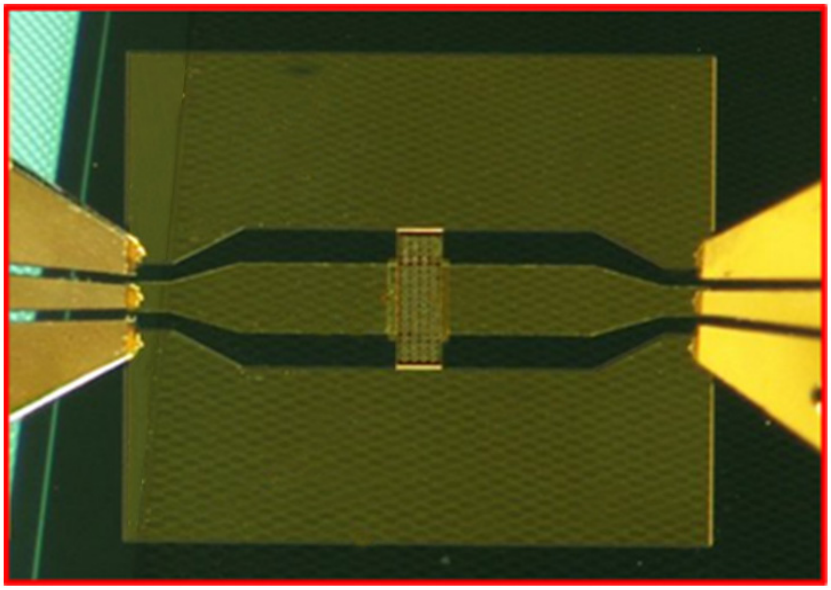

Fig. 17. Test-fixture structure of the RF MEMS switch manufactured by means of SU-8 photo-lithography. The input and output ports are connected to a vector network analyzer by means of coplanar probes for on-wafer characterization.

A further confirmation of the influence of the developed technological processing, and specifically the contribution from the gold stiffness, is evidenced from the mechanical response simulation plotted in Fig. 18 for a laterally actuated beam. In that case, the imposed residual stress is σ = 60 MPa, leading to two major effects: (i) the increase of the actuation voltage up to values greater than 90 volt, and (ii) a deformation of the bridge, which results in a more rigid shape.
It is worth noting that, looking at the shape of the bridge predicted in Fig. 18, an easier and more uniform actuation in the central part by using the lateral pads could be obtained because of the higher residual stress. On the other hand, the price to be payed in terms of the increase in the actuation voltage is not acceptable for many applications, and a trade-off has to be obtained, usually accounting for actuation voltages not exceeding 50 volt.
The only difference generated by changing the width of the bridge for the studied structure concerns with its RF response. Actually, the central capacitance defined by the bridge, the central conductor of the CPW and the dielectric between them changes the frequency of resonance for the device under test, while no change is recorded for the actuation voltages. Actually, wider beams experience lower frequencies of resonance when the switch is actuated and it works in isolation [56].
Further theoretical and experimental results have been obtained by using another shunt capacitive switch manufactured by using the silicon technology and developed at FBK-irst [57]. Top view and lateral dimensions of the device are shown in the following Fig. 19. The device is a clamped-clamped beam obtained on silicon wafer by means of an eight-mask sequence of technological steps, and the final release of the suspended bridge was obtained removing the sacrificial layer via an ashing process. The configuration is also characterized

by the following parameters: gap between bridge and floating metal g=2.85 μm, SiO_2 dielectric thickness on the central conductor of the CPW d=0.1 μm, beam thickness t=4 μm (grown by electroplating). By using the above values and those given in Fig. 19, we get an actuation voltage V=40 V ca. for the lateral actuation. The experimental value was V_{exp}=(41±2) V by using ten devices measured onto the same wafer in different positions

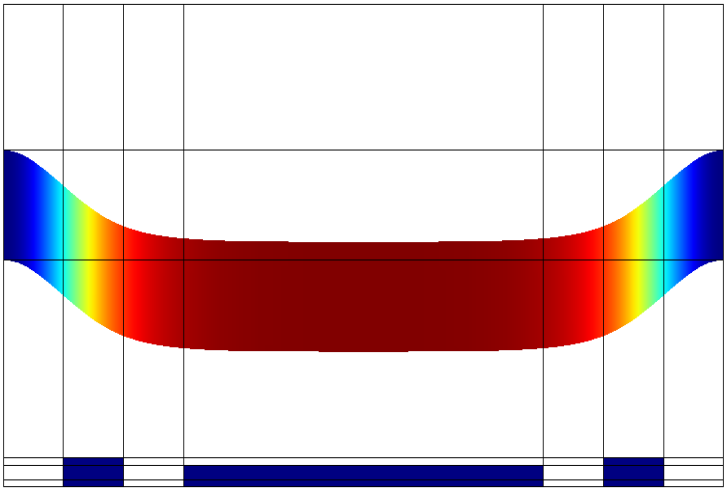

Fig. 18. Simulated deformation for the same bridge experimentally tested with a higher value of the residual stress (σ=60 MPa). An actuation voltage around 95 volt has been predicted.

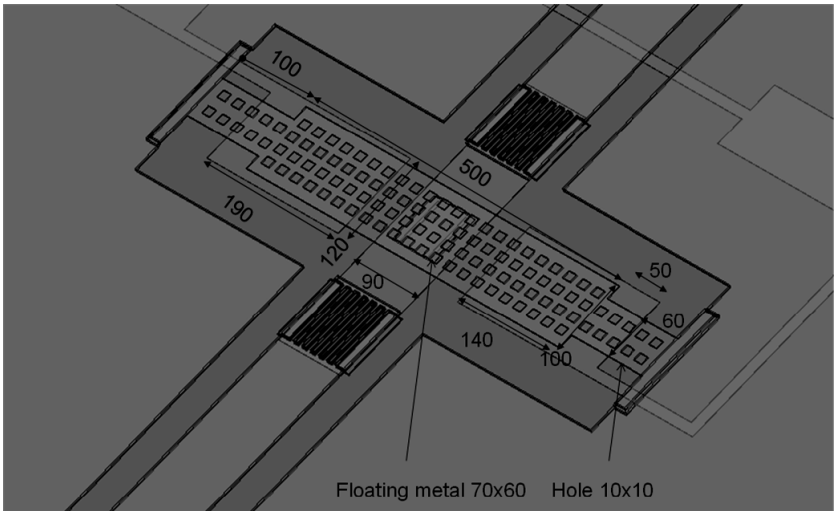

Fig. 19. Shunt capacitive switch manufactured by means of the eigth mask process developed at FBK-irst. Dimensions are in μm.

8. Conclusion

Analytical and numerical modelling for the mechanical response of a shunt capacitive RF MEMS switch have been compared by using an uni-dimensional theory, and 2D and 3D simulations performed by means of a commercial software package (COMSOL Multiphysics). Two actual configurations have been experimentally studied to validate the proposed model.
As a result, it has been demonstrated that RF MEMS mechanics can be predicted in a convenient way by uni-dimensional phenomenological models if evaluations about switching times, threshold voltage and preliminary dynamics have to be studied, without involving cumbersome simulations with a computer. In fact, the most part of the previous quantities depend on the equations to be used for the correct definition of the spring constant, and we demonstrated that the analytical approach based on the knowledge of the materials and of the geometry fulfils the most part of the quantities to be obtained. The actuation velocity and the switching times have been also defined and predicted by means of the analytical approach based on the Mechanical Energy considerations, including the applied DC voltage.
2D and 3D simulations are really useful for configurations having a very peculiar shape, especially for combining mechanical and RF predictions, being based on the same geometry, and this will be very useful to get a figure of merit for the RF MEMS technology (not yet available) based on different input conditions. Concerning the evaluation of the actuation voltage, the main parameter to be defined is the residual stress of the structure, because it dramatically influences the mechanical response of the bridge. On the other hand, with the proper knowledge of the technology used, the evaluation can be easily based on the uni-dimensional approach by defining effective quantities for simple configurations. The relative influence of surface forces and charging contributions has been discussed, to demonstrate that, under proper geometrical and material constraints, only charging effects can be really responsible for un-reliable structures, and a very simple solution to prevent this contribution is to tailor the switch in order to have contact-less actuation pads.

9. Acknowledgment

The activity has been partially funded by the ESA/ESTEC Contract on “High Reliability MEMS Redundancy Switch” ESA ITT AO/1-5288/06/NL/GLC contract No.20847

10. References

[1] G. M. Rebeiz and J. P. Muldavin: "RF MEMS Switches and Switch Circuits", *IEEE Microwave Magazine*, Vol.2, No.4, pp.59-71 (2001).
[2] G. M. Rebeiz, Guan-Leng Tan and J. S. Hayden: "RF MEMS Phase Shifters, Design and Applications", *IEEE Microwave Magazine*, Vol.3, No.2, pp.72-81 (2002)
[3] G. M. Rebeiz, “*RF MEMS, Theory, Design and Technology*”, John Wiley and Sons, Hoboken, 2003.
[4] Harrie A.C. Tilmans: “MEMS components for wireless communication”, *invited paper at XVI Conference on Solid State Transducers*, Prague, Czech Republic, Sept. 15-18, 2002
[5] E.K. Chan, E.C. Kan and R.W. Dutton: “Nonlinear Dynamic Modeling of Micromachined Switches”, *Proceed. Of IEEE MTT-Symposium*, pp.1511-1514 (1997).

[6] E.K. Chan and R.W. Dutton: "Effect of Capacitors, Resistors and Residual Charge on the static and dynamic Performance of Electrostatically Actuated Devices", *SPIE Symposium on Design and Test of MEMS/MOEMS* - March 1999.

[7] D. Mercier, P. Blondy, D. Cros and P. Guillon: "An Electromechanical Model for MEMS Switches", *Proceed. Of IEEE MTT-Symposium*, pp.2123-2126 (2001).

[8] G. De Pasquale, T. Veijola, and A. Somà, "Gas Damping Effects on Thin Vibrating Gold Plates: Experiment and Modeling", *Proceed. of DTIP 2009 Conference*, Roma, 1-3 April 2009, EDA Publishing/DTIP 2009, ISBN:978-2-35500-009-6, pp. 23-28 (2009).

[9] T. Veijola, "Compressible Squeeze-Films in Vibrating MEMS Structures at High Frequencies", *Proceed. of DTIP 2009 Conference*, Roma, 1-3 April 2009, EDA Publishing/DTIP 2009, ISBN:978-2-35500-009-6, pp. 235-238 (2009).

[10] T. Veijola, "3D FEM Simulations of Perforated MEMS Gas Dampers", *Proceed. of DTIP 2009 Conference*, Roma, 1-3 April 2009, EDA Publishing/DTIP 2009, ISBN:978-2-35500-009-6, pp. 243-250 (2009).

[11] P G Steeneken, Th G S M Rijks, J T M van Beek, M J E Ulenaers, J De Coster and R Puers, *Journal of Micromechanics and Microengineering* 15, 176 (2005).

[12] G. De Pasquale, A. Somà, Dynamic identification of electrostatically actuated MEMS in the frequency domain, *Mechanical Systems and Signal Processing, Volume 24, Issue 6, August 2010, Pages 1621-1633.*

[13] R.M. Lin, W.J. Wang, "Structural dynamics of microsystems—current state of research and future directions", *Mechanical Systems and Signal Processing, Volume 20, Issue 5, July 2006, Pages 1015-1043*

[14] P. Castellini, M. Martarelli, E.P. Tomasini, "Laser Doppler Vibrometry: Development of advanced solutions answering to technology's needs", *Mechanical Systems and Signal Processing, Volume 20, Issue 6, August 2006, Pages 1265-1285.*

[15] Matthew S. Allen, Michael W. Sracic, "A new method for processing impact excited continuous-scan laser Doppler vibrometer measurements", *Mechanical Systems and Signal Processing, Volume 24, Issue 3, April 2010, Pages 721-735*

[16] J. B. Muldavin and G. M. Rebeiz, "Nonlinear Electro-Mechanical Modeling of MEMS Switches", *Proceed. of IEEE MTT Symposium*, pp.21119-2122 (2001).

[17] Fuqian Yang, "Electromechanical Instability of Microscale Structures", *J. Appl. Phys*, Vol. 92, No. 2, pp.2789-2794 (2002)

[18] Z. J. Guo, N. E. Mc Gruer and G. G: Adams, "Modeling, simulation and measurement of the dynamic performance of an ohmic contact, electrostatically actuated RF MEMS switch", *J. Micromech Microeng.*, Vol. 17, pp.1899-1909 (2007)

[19] F. Michael Serry, Dirk Walliser and G. Jordan Maclay, "The role of the Casimir effect in the static deflection and stiction of membrane strips in microelectromechanical systems (MEMS)", *J. Appl. Phys.*, Vol. 84, No. 5 pp. 2501-2506 (1998)

[20] Steve K. Lamoreaux, "Casimir Forces: Still surprising after 60 years", *Physics Today*, February 2007, pp.40-45 (2007)

[21] Karl M. Strohm et al., "RF-MEMS Switching Concepts for High Power Applications", *Proceed. of 2001 IMS*, pp.42-46 (2001).

[22] B. Pillans, J. Kleber, C. Goldsmitht, M. Eberly, *Proceedings of the 2002 IEEE MTT-Symposium* 329 (2002).

[23] E.P. McErlean, J.-S. Hong, S.G. Tan, L. Wang, Z. Cui, R.B. Greed and D.C. Voyce, *IEE Proceedings on Microwave Antennas Propagation*, 152, 449 (2005).

[24] D. Dragoman, M. Dragoman, and R. Plana, *J. Appl. Phys.* 105, 014505 (2009).

[25] Brusa, E.; Munteanu, M.G.: "Role of nonlinearity and chaos on RF-MEMS structural dynamics", *Symposium on Design, Test, Integration & Packaging of MEMS/MOEMS, 2009. MEMS/MOEMS*. Volume , Issue , 1-3 April 2009 Page(s):323 - 328

[26] J. B. Muldavin and G. M. Rebeiz, "High-Isolation CPW MEMS Shunt Switches – Part 1: Modeling", *IEEE Trans. Microwave Theory and Tech*, Vol. 48, No. 6, pp.1043-1052 (2000).

[27] Romolo Marcelli, Giancarlo Bartolucci, Gianluca Minucci, Benno Margesin, Flavio Giacomozzi, and Francesco Vitulli: "Lumped Element Modelling of Coplanar Series RF MEMS Switches", *Electronics Letters*, Vol.40, No.20, pp.1272-1273 (2004)

[28] Giancarlo Bartolucci, Romolo Marcelli, Simone Catoni, Benno Margesin, Flavio Giacomozzi, Viviana Mulloni, Paola Farinelli: "An Equivalent Circuital Model for Shunt Connected Coplanar RF MEMS Switches", *Journal of Applied Physics*, Vol. 104, No. 8, pp.84514-1 - 84514-8, ISSN: 0021-8979 print+online (2008).

[29] Dimitrios Peroulis, Sergio P. Pacheco, Kamal Sarabandi, and Linda P. B. Katehi, "Electromechanical Considerations in Developing Low-Voltage RF MEMS Switches", *IEEE Trans. Microwave Theory and Tech*, Vol. 51, No. 1, pp.259-270 (2003).

[30] P. Arcioni et al., "Mastering Parasitics in Complex MEMS Circuits", *Proceed. Of the 35th European Microwave Conference*, pp. 943-946 (2005).

[31] M. Farina and T. Rozzi "A 3-D Integral Equation-Based Approach to the Analysis of Real-Life MMICs-Application to Mcroelectromechanical Systems", *IEEE Trans. On Microwave Theory and Tech.*, Vol. 49, No. 12, pp. 2235-2240 (2001).

[32] D. Girbau, N. Otegi and Lluis Pradell, "Study of Intermodulation in RF MEMS Variable Capacitors", *IEEE Trans. On Microwave Theory Tech.*, Vol. 54, No. 3, pp. 1120-1130 (2006).

[33] http://en.wikipedia.org/wiki/Young's_modulus

[34] C. Goldsmith, D. Forehand, D. Scarbrough, I. Johnston, S. Sampath, A. Datta, Z. Peng, C. Palego, and J.C.M. Hwang, *Proceedings of the IEEE 2009 MTT-Symposium*, 1229 (2009).

[35] Balaji Lakshminarayanan, Denis Mercier, and Gabriel M. Rebeiz "High-Reliability Miniature RF-MEMS Switched Capacitors", *IEEE Trans. on Microwave Theory and Tech.*, Vol.56, No. 4, pp.971-981 (2008).

[36] A. Koszewski, F. Souchon and D. Levy, Procedia Chemistry 1, 626 (2009).

[37] V.L. Rabinov, R.J. Gupta, S.D. Senturia, *Proceedings of the Int. Conf. On Solid – State Sensors and Actuators*, Chicago IL, June, 1997, 1125 (1997).

[38] Anna Persano, Fabio Quaranta, Adriano Cola, Antonietta Taurino, Giorgio De Angelis, Romolo Marcelli, and Pietro Siciliano: "Ta_2O_5 Thin films for Capacitive RF MEMS Switches", *J. of Sensors*, Hindawi Publishing, Volume 2010, Article ID 487061, 5 pages. doi:10.1155/2010/487061

[39] Y. Zhu, H. D. Espinosa, *Int. J. RF and Microwave CAE* 14, 317 (2004).

[40] X. Rottenberg, R. P. Mertens, B. Nauwelaers, W. De Raedt, and H. A. C. Tilmans, *J. Micromech. Microeng*. 15, S97 (2005).

[41] E. Papandreou, M. Lamhamdi, C.M. Skoulikidou, P. Pons, G. Papaioannou, and R. Plana: "Structure dependent charging process in RF MEMS capacitive switches", Microelectronics Reliability Volume 47, Issues 9-11, September-November 2007, Pages 1812-1817, *18th European Symposium on Reliability of Electron Devices, Failure Physics and Analysis*

[42] C. Kittel, *Introduction to Solid State Physics*, John Wiley and Sons Inc., 1996
[43] Lei L. Mercado, Shun-Meen Kuo, Tien-Yu Tom Lee, Lianjun Liu: "A Mechanical Approach to Overcome RF MEMS Switch Stiction Problem", *Proceed. of the 2003 Electronic Components and Technology Conference*, pp.377-384.
[44] Romolo Marcelli, George Papaioannu, Simone Catoni, Giorgio De Angelis, Andrea Lucibello, Emanuela Proietti, Benno Margesin, Flavio Giacomozzi, François Deborgies: *"Dielectric Charging in Microwave Micro-electro-mechanical Ohmic Series and Capacitive Shunt Switches"*; IOP Journal of Applied Physics, Vol. 105, No. 11, pp.114514-1 - 114514-10 (2009).
[45] C. H. Mastrangelo, "Adhesion-Related Failure Mechanisms in Micromechanical Devices", *Tribology Letters*, 1997, http://citeseer.ist.psu.edu/467772.html
[46] Patent http://www.patentstorm.us/patents/5772902.html
[47] E. Buks and M.L. Roukes, "Stiction, Adhesion Energy, and the Casimir Effect in Micromechanical Systems", *Phys. Rev. B*, Vol. 63, pp.33402-1 – 33402-4 (2001).
[48] G. Guisbiers, E. Herth, B. Legrand, N. Rolland, T. Lasri, L. Buchaillot, Materials selection procedure for RF-MEMS, *Microelectronic Engineering*, *Volume 87, Issue 9*, *November 2010*, *Pages 1792-1795*
[49] Brian Stark: "MEMS Reliability Assurance Guidelines For Space Applications", *Jet Propulsion Laboratory Publication 99-1*, Pasadena, California (1999).
[50] Peroulis, D. Pacheco, S.P. Katehi, L.P.B.: "RF MEMS switches with enhanced power-handling capabilities", *IEEE Trans. On Microwave Theory and tech.*, Vol. 52, No.1, pp. 59-68 (2004).
[51] S. Melle, D. De Conto, L. Mazenq, D. Dubuc, B. Poussard, C. Bordas, K. Grenier, L. Bary, O. Vendier, J.L. Muraro, J.L. Cazaux, R. Plana, "Failure Predictive Model of Capacitive RF-MEMS", *Microelectronics Reliability*, Vol. 45 pp.1770–1775 (2005).
[52] J. Franclov´a, Z. Kuˇcerov´a, and V. Burˇs´ıkov´, "Electrical Properties of Plasma Deposited Thin Films", *WDS'05 Proceedings of Contributed Papers, Part II,* pp.353–356 (2005).
[53] J. Iannacci, A. Repchankova, A. Faes, A. Tazzoli, G. Meneghesso, Gian Franco Dalla Betta, Enhancement of RF-MEMS switch reliability through an active anti-stiction heat-based mechanism, *Microelectronics Reliability*, *Volume 50, Issues 9-11*, *September-November 2010*, *Pages 1599-1603*
[54] M. Matmat, K. Koukos, F. Coccetti, T. Idda, A. Marty, C. Escriba, J-Y. Fourniols, D. Esteve, Life expectancy and characterization of capacitive RF MEMS switches, *Microelectronics Reliability*, *Volume 50, Issues 9-11*, *September-November 2010*, *Pages 1692-1696*
[55] http://www.comsol.com/
[56] A. Lucibello, E. Proietti, S. Catoni, L. Frenguelli, R. Marcelli, G. Bartolucci, Proceedings. of the Int. Semiconductor Conference CAS 2007, Sinaia, Romania, October 2007, 259 (2007).
[57] http://www.fbk.eu